

# EXPERIMENTAL INVESTIGATION OF DYNAMIC FRACTURE TOUGHNESS IN DCB SPECIMEN

*By*

Lovi Raj Gupta

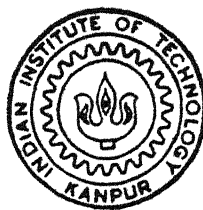
ME

1993

M

GUP

EXP



DEPARTMENT OF MECHANICAL ENGINEERING

INDIAN INSTITUTE OF TECHNOLOGY KANPUR

FEBRUARY, 1993

# **EXPERIMENTAL INVESTIGATION OF DYNAMIC FRACTURE TOUGHNESS IN DCB SPECIMEN**

A Thesis Submitted  
in Partial Fulfillment of the Requirements  
for the Degree of

**MASTER OF TECHNOLOGY**

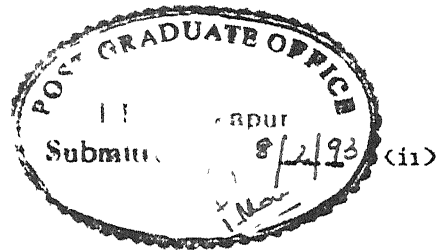
**by**

**LOVI RAJ GUPTA**

**to the**

**DEPARTMENT OF MECHANICAL ENGINEERING  
INDIAN INSTITUTE OF TECHNOLOGY  
KANPUR**

**FEBRUARY, 1993.**



## CERTIFICATE

It is certified that the work contained in the thesis entitled " EXPERIMENTAL INVESTIGATION OF DYNAMIC FRACTURE TOUGHNESS IN DCB SPECIMEN ", by " LOVI RAJ GUPTA ", has been carried out under our supervision and that this work has not been submitted elsewhere for a degree

*NN Kishore*  
Dr NN Kishore

Professor

Dept of Mech Engg

IIT, Kanpur

February, 1993.

*P. Kumar*  
Dr Prashant Kumar

Professor

Dept of Mech Engg

IIT, Kanpur

20 FEB 1973

CENTRAL 1 02100

1.14805

ME-1883-M-GUP-EXP



## ACKNOWLEDGMENTS

I am extremely grateful to Dr Prashant Kumar and Dr NN Kishore for their valuable and invigorating guidance through out this work. While looking back, I realize that without their constant encouragement and inspiration I could not have surmounted the difficulties during the present research.

Mr SK Verma deserves an accolade for teaching me to see things the way they are. At times, his genuine pieces of advice have helped me get out of my blues.

I am extremely grateful to Mr SC Gupta, Mr BD Pandey, Mr A Goel, Mr R Tiwari and all my friends in the ESA lab who continually assisted me in my experimental work. I am also grateful to Mr BK Jain of material science lab for extending all cooperation during my research.

It is with great pleasure, I recall my association with Deepak Gupta, Ajay Kumar, Anil Gupta and Satish Singh. I owe equal debts to all of them for extending gregarious companionship and moral support during my sojourn at IIT Kanpur.

I am indebted to my parents, my wife Vaishali and my son Mahim Raj for extending all cooperation and wishes bestowed by them.

-- LOVI RAJ GUPTA

## CONTENTS

CERTIFICATE	(ii)
ACKNOWLEDGEMENTS	(iii)
CONTENTS	(iv)
LIST OF FIGURES	(vii)
LIST OF TABLES	(viii)
NOMENCLATURE	(ix)
ABSTRACT	(x)

CHAPTER	1	INTERLAMINAR SIF IN DCB SPECIMEN UNDER QUASI-STATIC LOADING	
1 1		INTRODUCTION	1
1 1 1		Problems of interlaminar toughness	1
1 1 2		Literature Survey	2
1 1 3		Work done in this study	6
1 2		EXPERIMENTAL TECHNIQUES	7
1.2 1		Prelude	7
1 2 2		Specimen preparation and geometry	8
1 2 3		Bonding and precrack	10
1 2 4		Bonding of strain Gauges	13
1 2 5		Measurement of strain	18
1 2 6		Procedure	18

1 3	RESULTS	21
1 3 1	Introduction	21
1 3 2	Experimental Results	25
1 4	CLOSURE	27
CHAPTER 2	DYNAMIC INTERLAMINAR STRESS INTENSITY FACTOR	
2 1	INTRODUCTION	29
2 1 1	Prelude	29
2 1 2	Literature Survey	30
2 1 3	Out line of the present work	33
2 2	EXPERIMENTAL TECHNIQUES	34
2 2 1	Introduction	34
2 2 2	Specimen preparation	34
2 2 3	Preparation and usage of system which imparts high velocity to interlaminar crack	36
	Prenotched Bolt	
	Arch	
	Arch Aligning fixture	
	Assembly	
	Procedure	
2 2 4	Bonding of strain gauges	42
2 2 5	Measurement of strain	44
2 3	RESULTS AND DISCUSSION	46

2 3 1	Introduction	46
2 3 2	Experimental Results	46
2 3 3	Comparision with Quasi-Static	52
2 3 4	Reasons for slow crack growth	
2 4	CONCLUSIONS AND SUGGESTIONS FOR FUTURE WORK	56
	REFERENCES	58

## LIST OF FIGURES

No.	Title	Page No.
11	A DCB specimen loaded in mode I	9
12	Details of a Hinge	11
13	DCB specimen bonding fixture	12
14	Schematic diagram of strain gauge	14
15	Strain gauge bonding fixture	16
16	Position and Orientation of strain gauges	17
17	Bridge circuit	19
18	Actual crack length	22
19	Experimentally recorded strain and load	24
21	A cantilever of DCB specimen	35
22	Schematic sketch to represent prenotched bolt	37
23	Arch	39
24	Arch aligning fixture	40
25	Details of assembly	41
26	Strain gauge mounting fixture	43
27	Experimentally recorded strain v/s time (LD1)	48
28	Experimentally recorded strain v/s time (LD2)	49
29	Experimentally recorded strain v/s time (LD3)	50
210	Experimentally recorded strain v/s time (LD4)	51

## LIST OF TABLES

No.	Title	Page No.
TABLE I	Experimentally observed peak strain and associated $K_{IC}$ for single and double strain gauges and comparison with numerical solutions	28
TABLE II	Variations in experimental and numerical values of $K_{IC}$ by Potty and Lovi	28
TABLE III	Experimentally observed Peak strain and associated $K_I^D$	55

## NOMENCLATURE

$a,l$	Crack length
$b$	Width of the cantilever of DCB specimen
$E$	Young's Modulus
$G$	Energy release rate
$G_{IC}$	Critical energy release rate in mode I
$G_{IIC}$	Critical energy release rate in mode II
$h$	Thickness of each strip of DCB specimen
$I$	Moment of Inertia
$K$	Stress intensity factor (SIF)
$K_{IC}$	Critical SIF in mode I
$K_{IIC}$	Critical SIF in mode II
$K_I^D$	Critical Dynamic SIF in mode I
$P$	Load applied to the end of DCB specimen
$U$	Elastic strain energy stored in the specimen
$\epsilon$	Strain at a point
$\delta$	Deflection in the arm of DCB specimen under load
$\nu$	Poisson's Ratio
$\sigma$	Stress at a point
$\mu\epsilon$	Micro-Strain

## ABSTRACT

The present work is performed to experimentally evaluate the stress intensity factors (SIF) under quasi-static crack growth and under dynamic crack growth conditions.

The work to determine quasi-static critical SIF was mainly concerned towards improving the technique which had already been developed but was having problems owing to inconsistency in result. In that technique, SIF was experimentally determined by taking a double cantilever beam (DCB) specimen made of slender steel cantilevers bonded together with epoxy. Strain near the crack tip was measured by bonding strain gauge only on the upper cantilever relating it to SIF through a FEM relation. The technique was providing inconsistent result owing to curvature developed in the DCB specimen during bonding the cantilevers. The strain gauge on the upper cantilever was not separating the strain due to curvature from the strain developed by the crack tip. The modifications to this are made in the present study by using a dual mirror image combination of strain gauges to measure the strain near the crack tip. The measured SIF is brought to a variation of 14-19% as compared to earlier variation of -15% to +55%. The average SIF for quasi-static tests determined through modified technique is 4.22 MPa $\sqrt{m}$ .

For experimentally evaluating the dynamic SIF a mechanism is developed to store strain energy in the arms of the DCB specimen loaded in mode I by clamping the two cantilevers



together with a prenotched bolt just prior to the crack tip. The cantilevers were pulled in a tensile loading machine so as to store predetermined strain energy in the cantilevers. This energy was then suddenly released to impart high velocity to the moving crack. Two sets of strain gauges were used to measure the strain time profile and crack velocity. In the experiments conducted, first set of strain gauges recorded expected strain pulses but the second set of strain gauges was unable to sense the strain pulse owing to low crack velocity. Based on strain time profile of the first set, average dynamic SIF was found to be 358 MPa $\sqrt{m}$ .

# CHAPTER I

## INTERLAMINAR SIF IN DCB SPECIMEN UNDER QUASI-STATIC CRACK PROPAGATION

---

### 1.1 INTRODUCTION

#### 1.1.1 Problems of interlaminar toughness

One of the main mechanisms of failure in composite materials subjected to impact loading is delamination. Delamination occurs due to poor interlaminar fracture toughness and the crack can propagate with a velocity as high as 300 m/s [1]. It is of great importance to measure the interlaminar fracture toughness of a composite material in order to improve its performance under impact loading.

Interlaminar fracture toughness is measured universally by using energy release rate ( $G$ ) for both mode I and mode II. This method adopts the technique of balancing energies in the specimen. The technique is acceptable for the static case, but in the case of dynamic energy release rate, an energy imbalance is found. The energy imbalance is caused because the fast moving crack emanates stress waves which encounter the flaws, kinetic energy gets converted to heat, which is

transferred to the specimen holder or the surroundings. Such transformation is also known as deformation friction [2]. This heat generation cannot be easily measured, thus resulting in inaccurate energy measurement. In the case of composites, the interlaminar energy release rate is very small, of the order of  $200 \text{ J/m}^2$ , as compared to some materials which have energy release rate as high as  $30,000 \text{ J/m}^2$ . Thus small inaccuracies in energy balance may lead to large variations in the experimental results. Another limitation of the energy release rate parameter is that it does not provide stresses, strains or displacement field in the vicinity of the crack tip. This restricts the measurement of stress and strain field near the crack tip. So considering these limitations in energy release rate approach, other techniques may be explored.

## 11.2 LITERATURE SURVEY

The critical energy release rate technique is developed and is used extensively. Wilkins et.al.[3] found critical strain energy release rate in delamination for mode I and mode II using a DCB specimen loaded quasi statically. Han and Koutsky [4] obtained the interlaminar fracture energy values in case of glass fiber reinforced polyester composites. Devile et.al. [5] developed a nonlinear theory for energy release rate using DCB specimen. Prasad [6] evaluated experimentally under dynamic loading conditions, the critical energy release rate in

mode I for glass fabric reinforced epoxy laminates and was not able to account for energy which was transformed into heat, Babu [7] also performed experiments and evaluated critical energy release rate for mode II in CFRP using a CNF (centered notch flexural) specimen but he was not able to measure the crack velocities accurately.

An expression for the critical intensity factor for mode I of a double cantilever beam specimen with thin cantilevers, loaded statically, is well known [8]. It adopts a method by first finding compliance,  $c$ , of the specimen and then finding the energy release rate ( $G$ ) by the formula

$$G = \frac{1}{2} \frac{P^2}{B} \frac{\delta c}{\delta a}$$

where,  $P$  is the load on the cantilever,  $a$  is the crack length and  $B$  is the width of the specimen. Regarding this as a case of plane strain  $K_I$  is then determined by using formula,

$$K_I = \sqrt{\frac{G_I E'}{(1-\nu)}}$$

Where  $\nu$  is the Poisons ratio. This method only gives value of stress intensity factor and ignores the strain field around the crack tip which is strongly influenced by

the nearby traction free surface

Williams [9] investigated the crack tip singularity at the interface of two materials. Through mathematical analysis he showed that if the materials at the interface are similar then a square root singularity exists, whereas, if the materials at the interface are different then the singularity in the vicinity of the crack tip has oscillatory character of the type  $r^{-1/2} \sin(b \log r)$  where  $b$  is a constant and  $r$  is the distance from the crack tip. This was carried out for a single edge notched (SEN) specimen.

Sih and Jih [10] developed analytical strain energy release rate for mode I and mode II, using numerical and finite element methods. It was computed for a crack lying along the interface of two dissimilar elastic media. The analytical solutions indicate that  $G_I$  and  $G_{II}$  do not converge in the form of crack closure integral although the sum (i.e. the total strain energy release rate) is well defined. If the oscillatory terms are neglected, then  $G_I = G_{II} = \frac{1}{2}G$ .

Shukla, Agarwal and Bhushan [11] measured stress intensity factor of a crack in a large orthotropic SEN composite material. Theoretical equations were developed for strain field in the vicinity of the crack tip in an orthotropic material. These equations were then evaluated to obtain the optimum location and orientation of the strain gauges to be used for strain measurements. It was then verified experimentally in a single edge notched (SEN) specimen under quasi-static loading.

conditions

Nadarajah, Shukla and Letcher [12] conducted an experimental study to show the application of fiber optic sensors to fracture mechanics problems of through the thickness crack in a cantilever beam. Mode I stress intensity factors were obtained using single mode optical fibers in a single notched specimen fabricated from aluminum. A Mach-Zehnder interferometric set up was used during the experiments.

A technique has been recently developed to experimentally determine the stress intensity factor (SIF) in a double cantilever beam specimen with slender cantilevers through a scheme of measuring strain near the crack tip. The strain field of the DCB specimen is not available through a closed form solution. Analytical solution is difficult because the free surfaces are lying very close to crack plane. Therefore, a finite element software was developed by Verma et al [13] for finding strain field around the crack tip for computing stress intensity factor. The finite element program also helped in selecting the proper location of strain measurement and choosing the optimum orientation of the strain gauge. On these recommendations, Potty [14] conducted experiments on a DCB specimen made from two slender hardened steel plates bonded together by epoxy with a precrack. Then the strain gauge of extremely small gauge length (0.2mm) is bonded. When the quasi-static load is applied on the DCB specimen, the crack grows and passes under the strain gauge. Knowing the strain and using

the relation between SIF and strain, critical intensity factor (SIF) is determined. In this experimental investigations the results were not consistent because of residual strain developed in DCB specimen at the time of bonding.

### 1.3 WORK DONE IN THIS STUDY

The technique of Potty for finding critical SIF by measuring strain close to crack tip in a DCB specimen is improved in this study. So far only one strain gauge was used at an optimal location. Improvements in the method is carried out in this study using two strain gauges one on each cantilever. This is done so as to eliminate the effect the curvature formed in DCB specimen during bonding. The strains are then measured and the value of stress intensity factor is evaluated. The experimental results are then compared with values obtained numerically.

## 1.2 EXPERIMENTAL TECHNIQUES

### 1.2.1 PRELUDE

In the work of Verma et al [13] and Potty [14] stress intensity factor (SIF) in a double cantilever beam (DCB) specimen with slender cantilevers was determined through a combined scheme of measuring strain near the crack tip and then analyzing data by using an FEM program [13]. The DCB specimen was made from two slender steel cantilevers, bonded together by epoxy. The precrack was introduced during bonding by intruding a thin film of biaxially oriented poly-propylene (BOPP).

The strain field of a DCB specimen with slender cantilevers cannot be easily expressed through a closed form solution because the free surface is near the crack plane. Therefore, a finite element software by Verma et al [13] was developed for finding strain field around the crack tip for computing the SIF. The relation between measured strain in the vicinity of the crack tip and the stress intensity factor was established by the program. The program also gave the optimal location and orientation of the strain gauge.

The specimen was loaded in mode I under quasi-static load and displacement controlled conditions. The



strain in the vicinity of crack tip was measured by a very small strain gauge with 0.2 mm gauge length, bonded at an angle of  $45^\circ$  to the crack plane. The strain gauges were bonded at the mid plane of the corresponding cantilevers. The peak strain was then determined by a strain indicator and was then fed to the established relation of strain and SIF. The experimental and numerical values of critical stress intensity factor ( $K_{IC}$ ) were then compared. The measured value of  $K_{IC}$  was found to be lower than the numerical value.

The inconsistency in the value of the critical stress intensity factor measured experimentally and evaluated numerically was found because during bonding of the thin steel cantilevers, the assembly is found to have a curvature in spite of pre- and post- bonding precautions. This curvature initiates a residual strain in the DCB specimen which is not associated with the strains produced by the delamination crack, variation in experimental values of SIF is observed.

### 1.2.2 SPECIMEN PREPARATION AND GEOMETRY

The DCB specimen was used by Potty for his study has been adopted for this study. It has two slender metal strips. The thickness of each cantilever is 2.78 mm and the width is 24.0 mm (FIG 2.1)

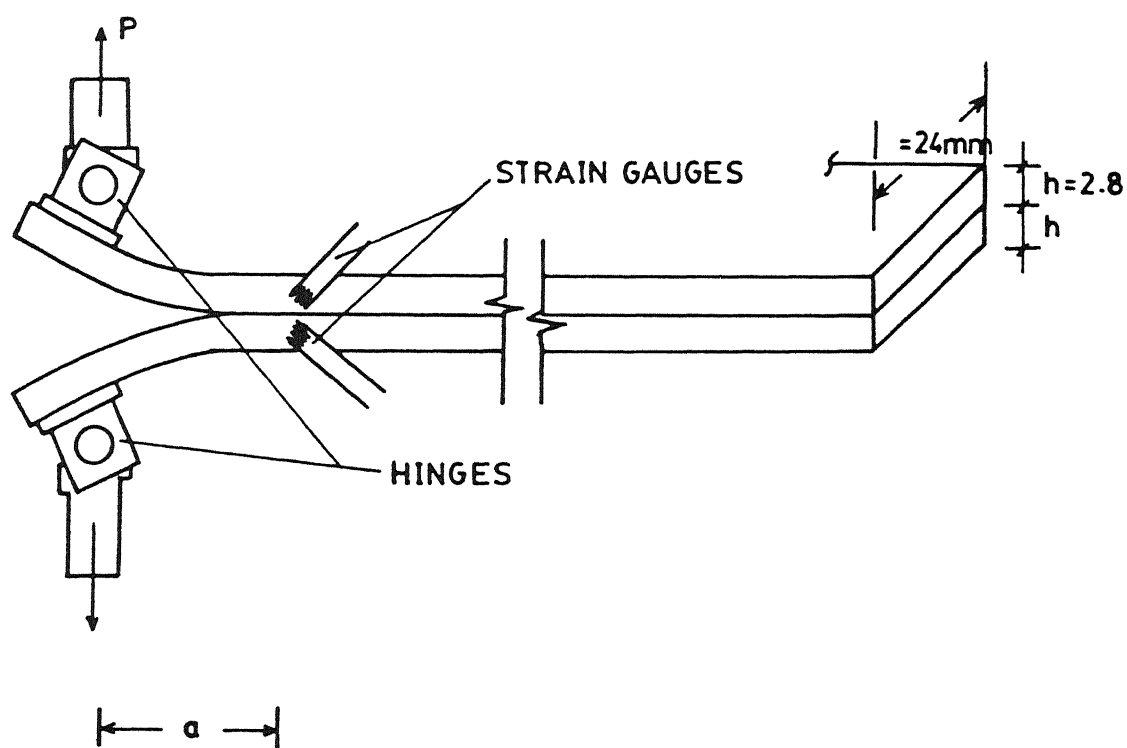


FIG 1.1 A DCB specimen loaded in mode I.

The material used was alloy steel 40Ni2Cr1Mo28 (EN24) hardened, by heating it to 830-850°C for one hour and then quenching it in the oil. This was followed by annealing at 310° C for 20 minutes, so as to relieve the residual stresses. The average hardness attained by each cantilever was 33 on C-scale corresponding to a yield stress of nearly 1000 MPa. Each strip was then grounded flat and its surface is prepared by rubbing on fine grit emery paper (Grade 220) for five minutes with light hand pressure.

A hinge consisting of a bracket, a support and a pin all made of steel was used at the load application point. The hinges keep the applied loads normal to surfaces and keeps the loads colinear for both the cantilevers (FIG 12). They also provide a degree of freedom to the cantilevers to rotate during their bending.

### 1.2.3 BONDING AND PRECRACK

The metal strips forming cantilevers of DCB specimen are bonded by epoxy LY 556 and hardener HY 1907IN in the ratio of 100 : 85 by weight. The faces to be bonded, are cleaned with acetone to degrease and remove dust particles. The mixture of epoxy and hardener is applied evenly and two strips are then put together in a fixture (FIG 13).

While bonding the cantilevers, a precrack is introduced by placing a film of BOPP up to required length

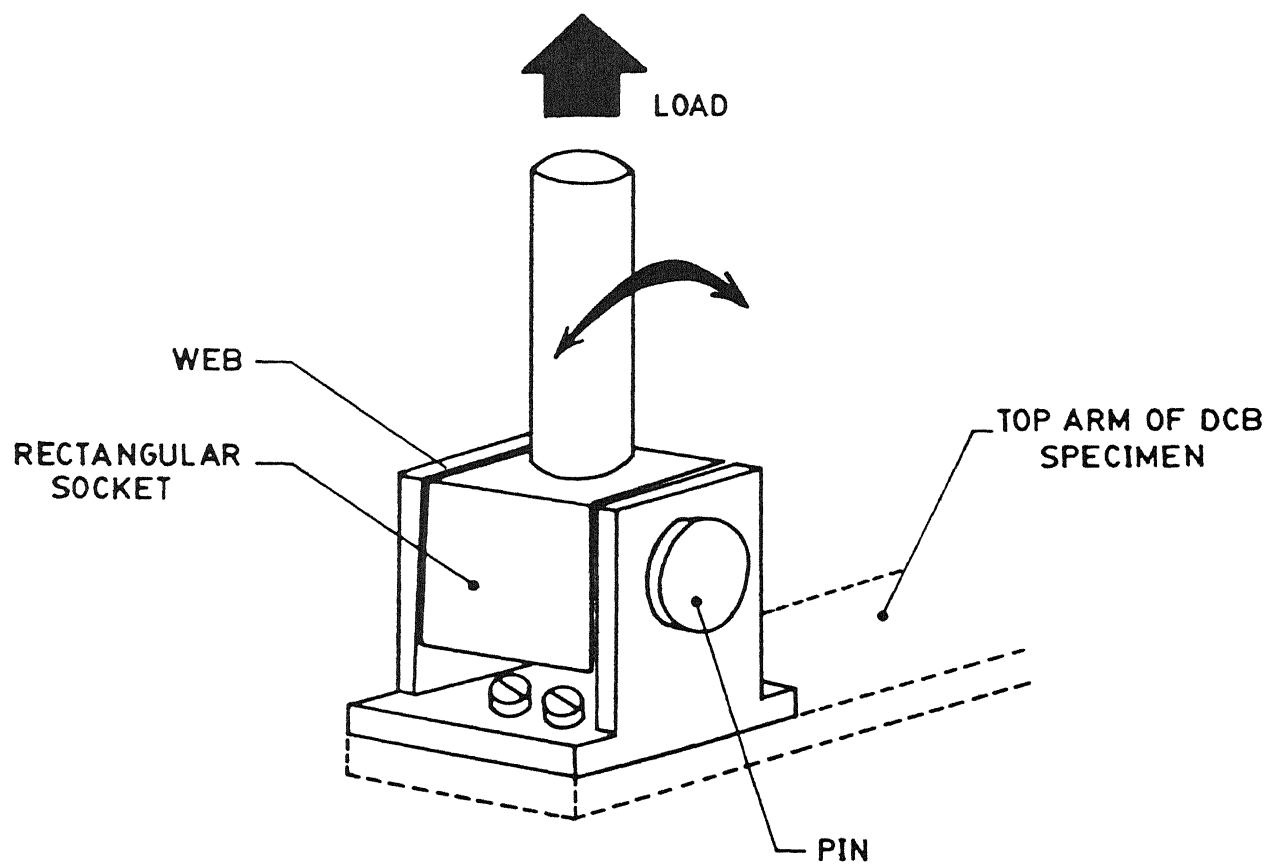


FIG 12 Details of a hinge.

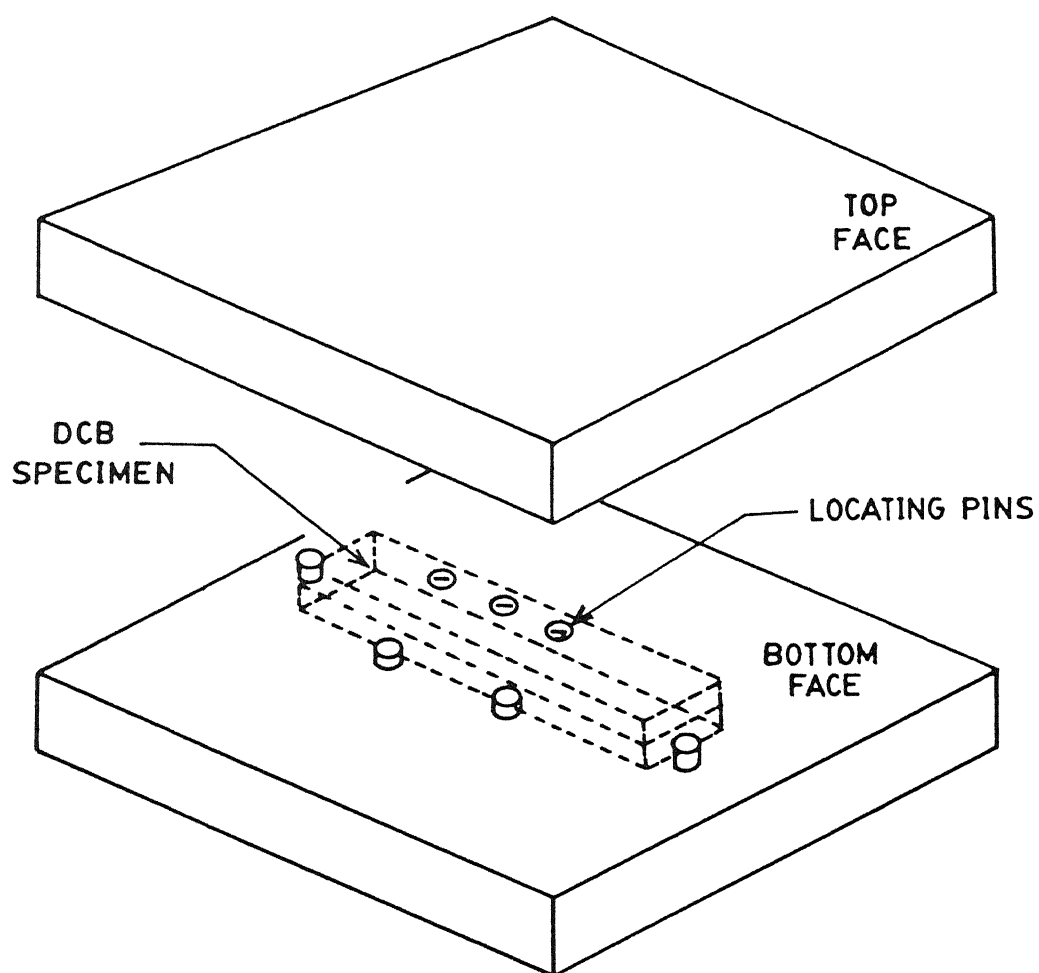


FIG. 1.3 DCB specimen bonding fixture.

BOPP restricts bonding a precrack is generated. In this study the precrack length was kept at 30.0 mm.

The fixture along with the specimen is placed between platens of a hydraulic press. The platens are heated through in built heaters and the temperature is monitored by placing a chromel-alumel thermocouple. The temperature of the specimen is maintained at  $130^{\circ}\text{C}$  under 12 MPa pressure for one hour.

A felt is placed on the top strip of the cantilever so as to evenly distribute the applied pressure. This is done to avoid formation of a localized pressure zone which results in uneven bonding.

#### 1.2.4 BONDING OF STRAIN GAUGES

This constitutes the major objective in the present work.

#### *STRAIN GAUGES*

The strain gauges in use are supplied by Tokyo Sokki Kenkyujo Co. Ltd., Japan. The gauges have a gauge length of 0.2 mm and a gauge width of 15 mm. The base of strain gauge is rectangular with dimensions 35 mm  $\times$  2.5 mm (FIG 14). Its resistance is  $120 \pm 0.3 \Omega$  and the gauge factor is, 2.07.

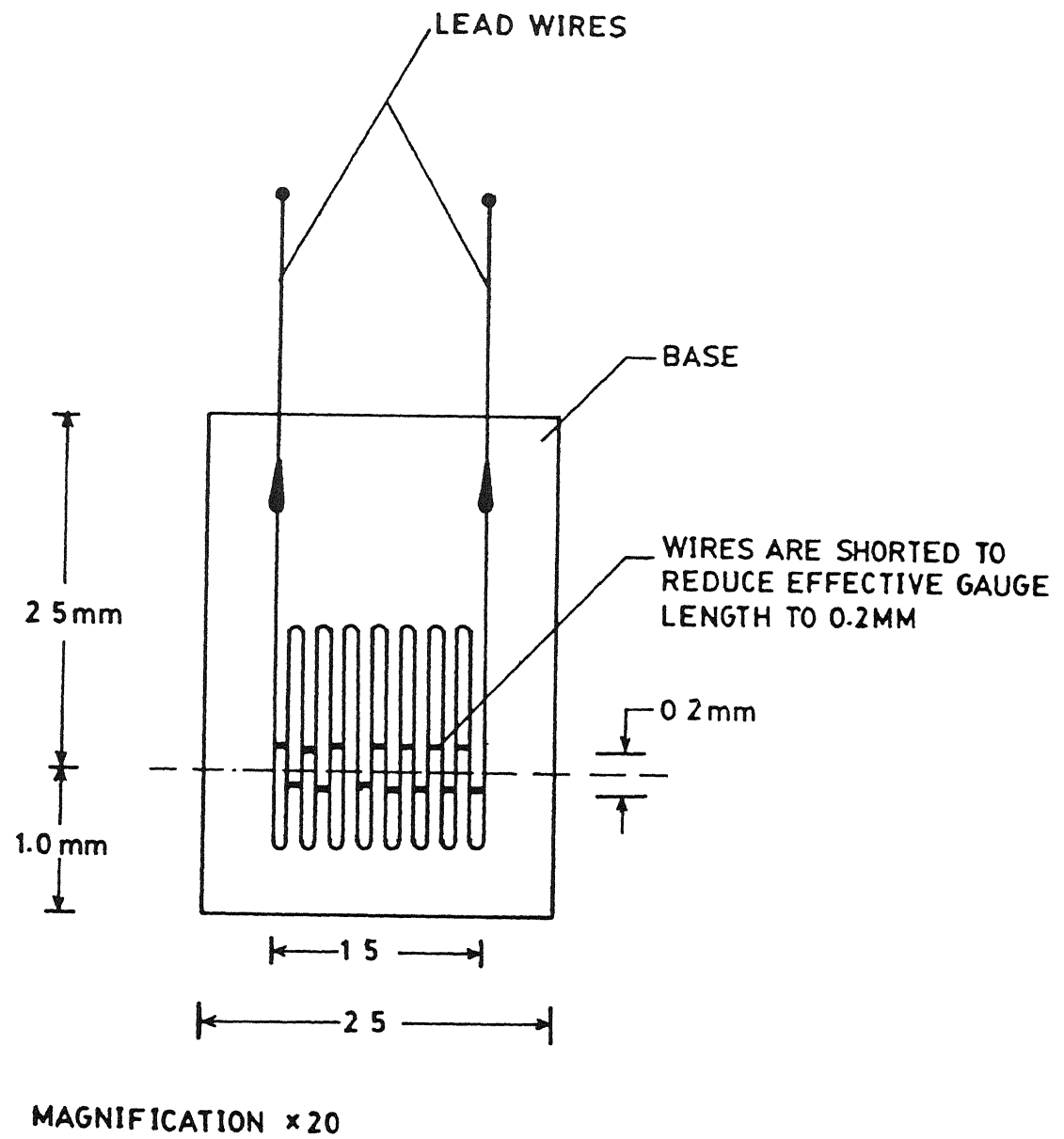


FIG. 1.4 Schematic diagram of Strain Gauge. Magnification 20

## BONDING OF STRAIN GAUGES

As the area on to which strain gauges are to be bonded is very small, extreme care is undertaken. Positioning of both the strain gauges are done with the help of a fixture. This fixture is made of two self sticking papers placed normal to each other so as to house a corner of the strain gauge in the top cantilever. For locating the strain gauge in the bottom cantilever, the hatched section of self sticking paper (FIG 15 ) is carefully cut off by a blade. The area lying under the fixture is thoroughly cleaned with acetone to degrease and remove dust particles. Epoxy LY 556 and the hardener HY 951 are used in the ratio 10 : 1 by weight. The ambient temperature is kept around 55 to 60 °C for about 24 hours to help curing. Localized pressure is also applied while curing takes place.

The mixture of epoxy and hardener is applied evenly and the strain gauges are then put over it. The assembly is then put under infra-red lamp, to attain the curing temperature, for 24 hours. The infra-red lamp also restricts the moisture in the vicinity of bonded strain gauges.

After the curing is over, to check the location and orientation, the bonded strain gauges are then placed under travelling microscope. Readings of microscope are taken and X, Y coordinates of the strain gauge base are recorded. Figure 16 shows a typical record of measurement. This plotted graph ensures the accuracy of the location and orientation of the



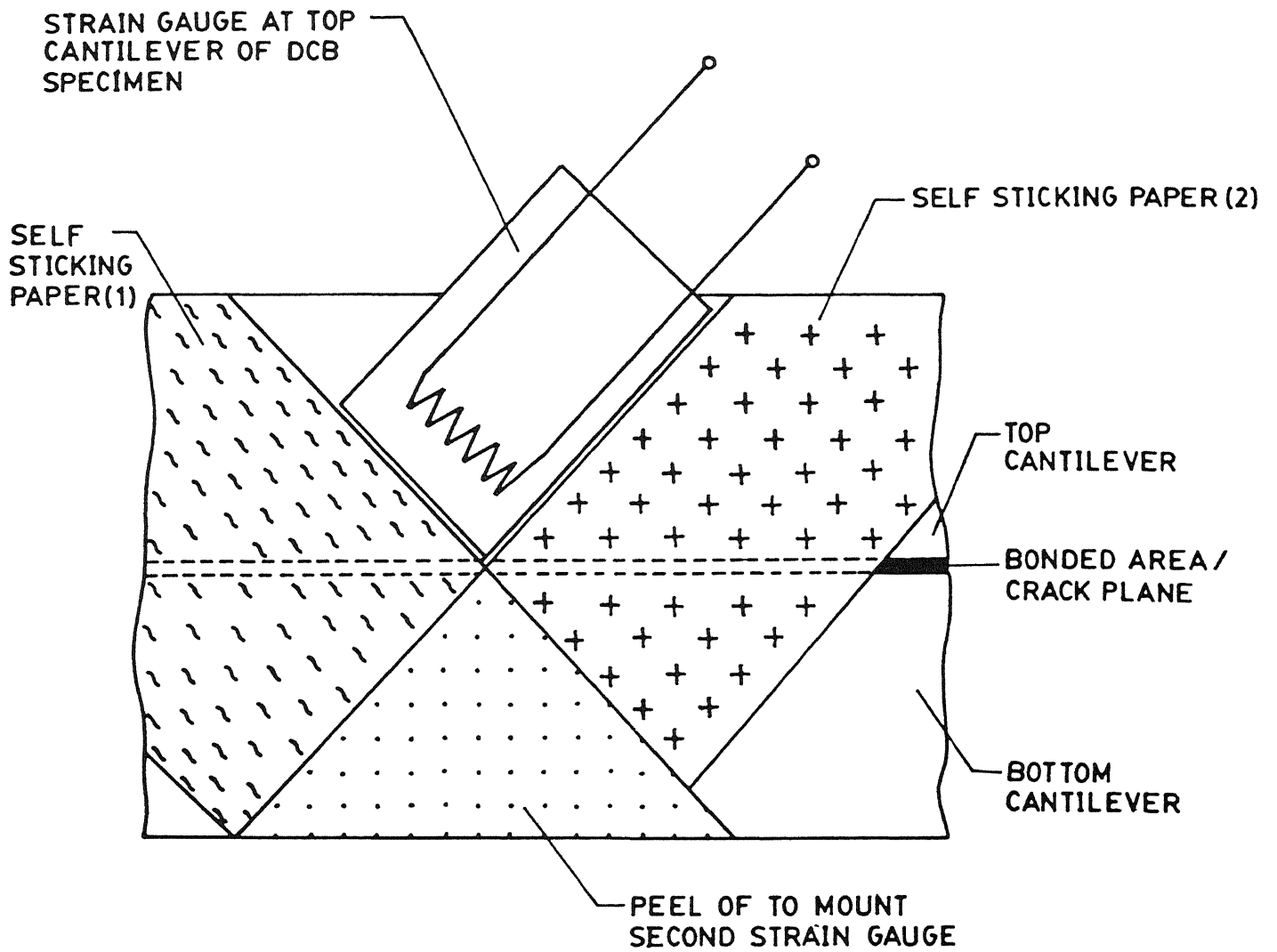


FIG 15 Strain Gauge bonding fixture made out of sticking paper.

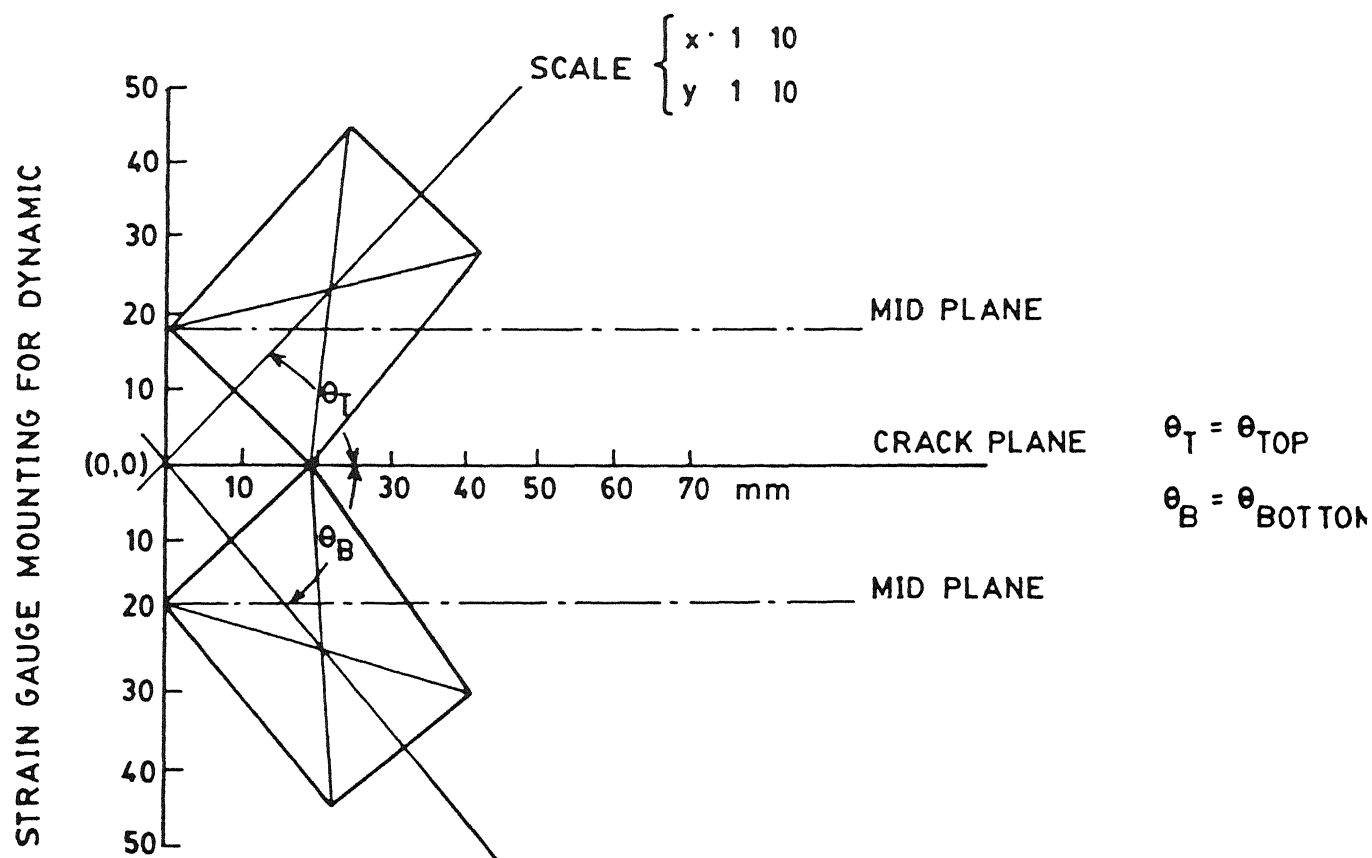


FIG. 1 6 Positioning and orientation of Strain Gauges recorded by the travelling microscope

strain gauges It is seen that the center of gauges are within 0.05mm from the prescribed location and the orientation is within  $\pm 2^\circ$

### 1.2.5 MEASUREMENT OF STRAIN

Two dummy strain gauges, both having resistance 120  $\Omega$  are used to complete the bridge (FIG 17 ). The strain gauge output is measured using strain indicator (Model P-350A, Measurement Group). The full bridge mode of strain indicator is used (FIG 18 ). The initial value of strain indicator is noted, and then the variations in the strain are recorded. The variation of strain is in the form of a spike i.e. it starts from zero, rises to peak and then dips down to zero. These are plotted to give the peak strain value.

### 1.2.6 PROCEDURE

The DCB specimen is mounted on INSTRON machine and the connecting wires of the strain gauge are tied and suspended by a thin thread to keep the axis of the specimen horizontal. The specimen is loaded in a displacement controlled mode, with the cross head speed fixed at 0.05 mm/min, and the full scale load 200 N. The chart speed for recording the graph

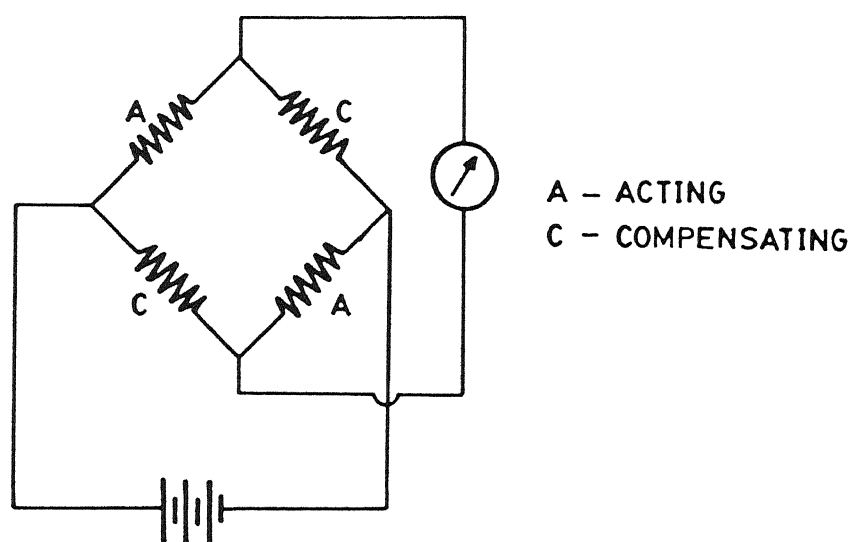


FIG 17 Bridge circuit

displacement versus load is maintained at 20 mm/min. In this machine, the upper jaw is fixed and the lower jaw moves the load is applied. Once the loading is started, the strain indicator readings are noted after regular intervals of time.

### 1.3 RESULTS

#### 1.3.1 INTRODUCTION

The precrack is intruded to 30 mm length during bonding of the cantilevers together and the strain gauges are bonded at 80 mm beyond the tip of the precrack. As found by the numerical analysis, the peak strain is encountered when the crack tip is at 15 mm prior to the strain gauges. Thus the actual crack length becomes 365 mm (FIG 18)

The DCB specimen is then loaded in mode I. As the load is increased, a stage is reached when the crack starts propagating. The propagation of crack is very slow and the strain output of the gauge is recorded with a strain indicator at regular intervals of time, setting the strain zero when the load is zero. The strain increases as the crack scoots near the strain gauges, reaching a peak.

The load applied at the ends of the cantilever is recorded through a strip chart recorder of the tensile testing machine. This chart gives load versus time curve. From this, load corresponding to peak strain is also determined.

Knowing the peak strain  $\epsilon_{\text{Peak}}$  and the peak load value (P), for a particular crack length (365mm)  $K_{IC}$  is

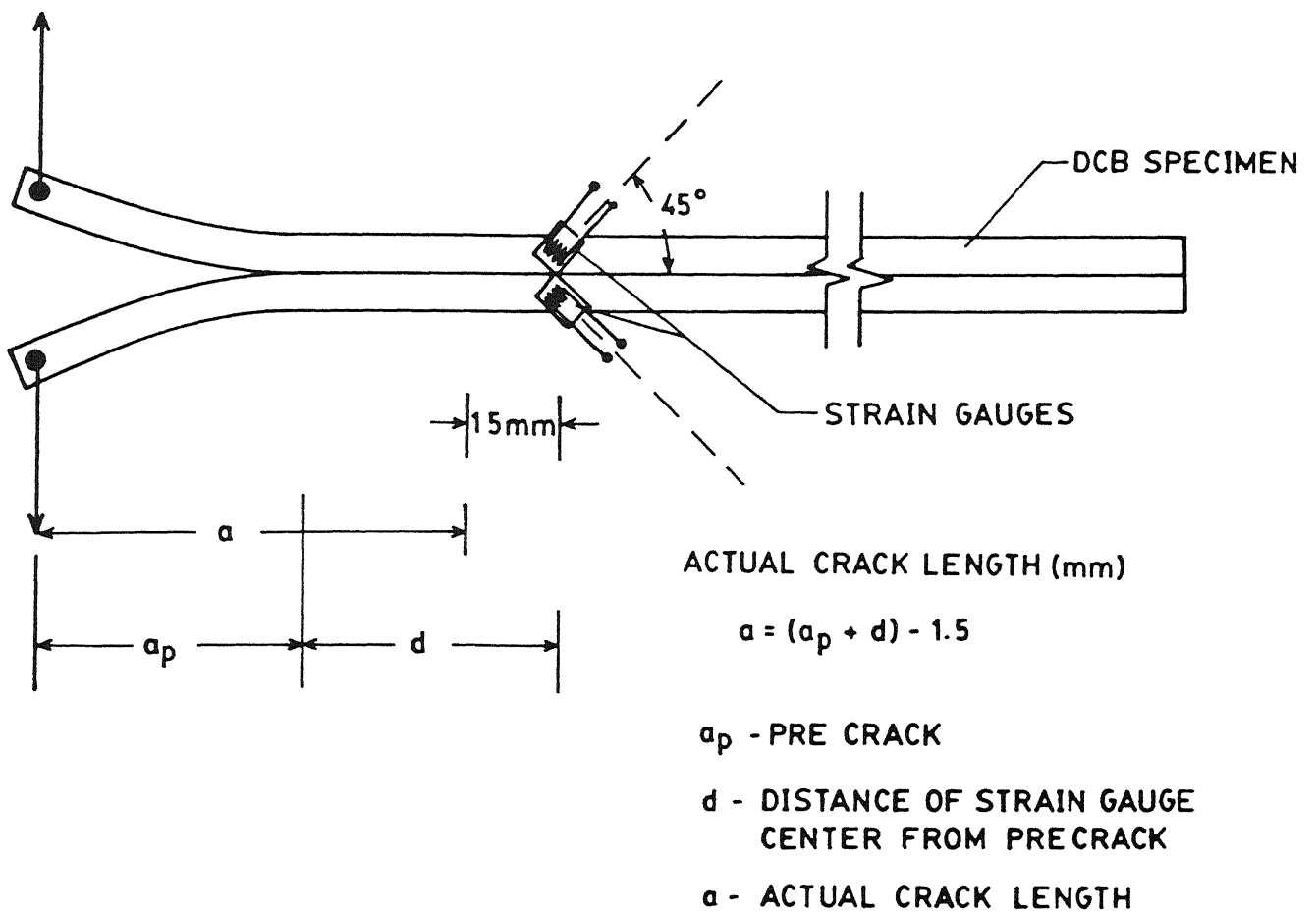


FIG. 1.8 Actual crack length

calculated

The experimental critical stress intensity factor  $K_{IC}^{exp}$  is evaluated by following relation. The relation is established for the given geometry of the DCB specimen through a finite element program [13]

$$K_{IC}^{exp} = 0.02423867 \times \epsilon_{Peak} \quad (3.1)$$

Knowing the load (P) corresponding to peak strain value for the given geometry of DCB specimen through finite element program a relation was established between the load and the critical intensity factor. The critical intensity factor in mode I, numerically is given by,

$$K_{IC}^{num} = 0.0329 \times P \quad (3.2)$$

The closed form solution are obtained analytically through energy release rate approach and the following relation gives the critical intensity factor through closed form solution

$$K_{IC}^{cf} = \frac{2\sqrt{3} \times P \times a}{h^{3/2} B (1-\nu^2)} \quad (3.3)$$

where  $\epsilon_p$  is the peak strain, P is the peak load, h is the thickness of the cantilever and B is the width of the cantilever



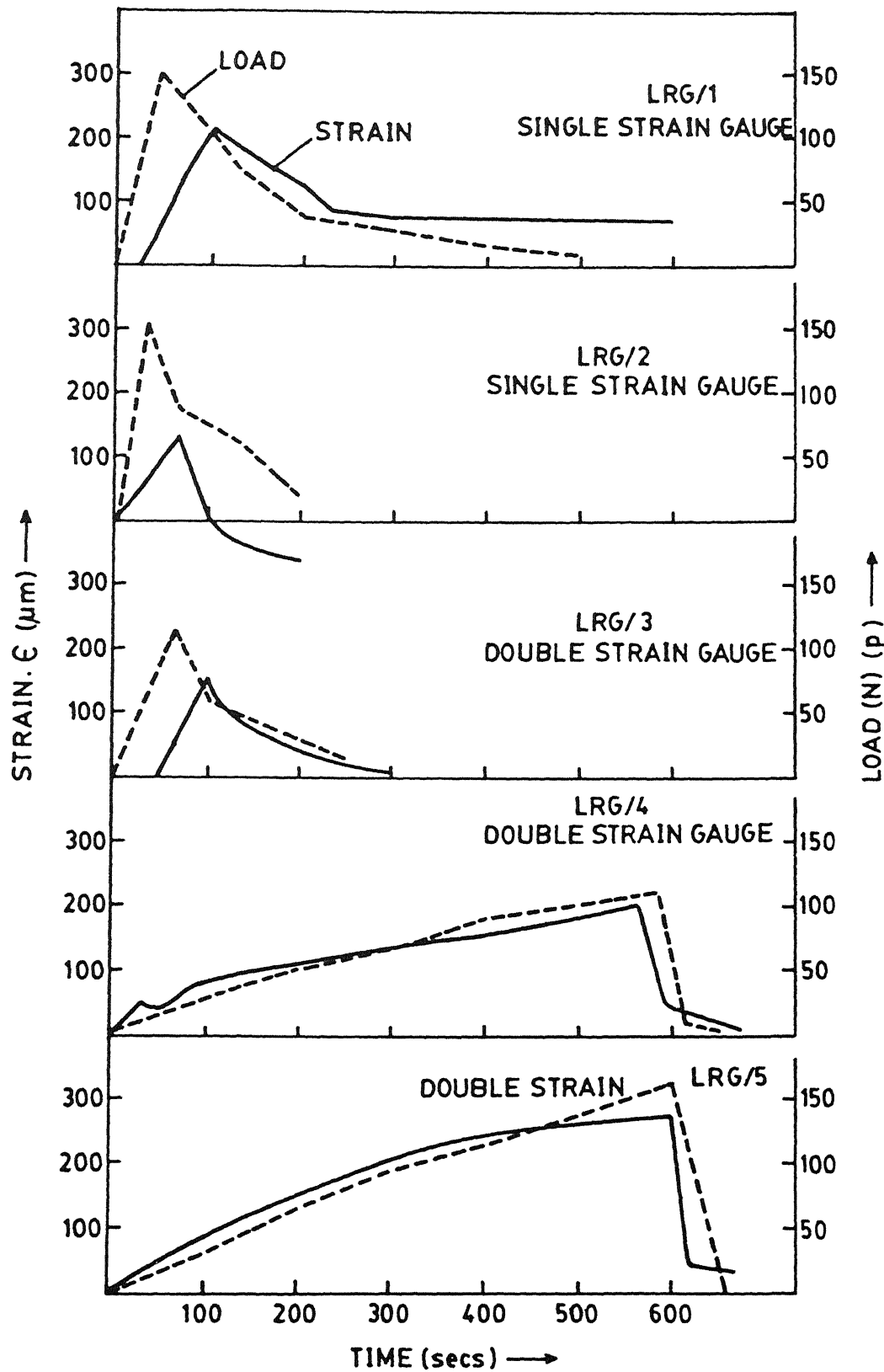


FIG. 1.9 Recorded strain (per strain gauge) and load at the end of Cantilever for cases of single and double strain gauges.

### 1.3.2 EXPERIMENTAL RESULTS

A total of five experiments were conducted in this study. Out of these five, two were done with single strain gauge and three were done with two strain gauges. In each experiment, load versus time and strain versus time were recorded and plotted FIG 19.

There is only one flaw associated with the use of a dual combination of strain gauge, that is, there are a number of wires coming out of gauges. They make it difficult to place the DCB specimen horizontally and tend to apply additional force. Special care should be taken to support the cables through a separate arrangement.

For explaining the results of the experiment, the observations of the LR6/2 (one strain gauge) and the LR6/3 (with two strain gauges) experiments are considered in detail. The strain at the end of experiment when the DCB specimen is unloaded should be zero because the strain gauge is placed at the neutral axis of the cantilever. In LR6/2 the residual strain is 52.35 % of the peak strain. The prestraining is due to the curvature developed in the specimen during bonding of the cantilevers. In LR6/3 the residual strain is 9.00 % of the peak strain. In the experiment LR6/3 the strain at the end became small because using two strain gauges the effect of curvature is canceled out. This signifies the use of two

strain gauges so as to eliminate the curvature adopted by the DCB specimen during bonding

In the figure 1.9 it is clear that when only one strain gauge was used the behavior of recorded strain was not satisfactory, but after using two strain gauges and canceling the effect of curvature in the DCB specimen the results were satisfactory. The peak strain and corresponding load values along with the  $K_{IC}$  through different approaches are tabulated in Table I. This table also provides the % variation in the experimental and numerical values of  $K_{IC}$ .

The variation seen in the experimental and numerical values of critical stress intensity factor by measuring strains near the crack tip, using single strain gauge is quite inconsistent i.e it varies from -18% to +75%. Whereas the variation using dual strain gauge combination is only between +15% to +19%. This can be seen in Table II.

Furthermore, the percentage variation of experimental and numerical values of  $K_{IC}$  using dual strain gauges is much much more consistent than the variation in experiments using a single strain gauge for measuring strain in the vicinity of crack.

#### 14 CLOSURE

In the present study, the combination of dual, mirror image strain gauges is used in place of single strain gauge in the vicinity of the crack tip. It is observed that the use of a dual, mirror image combination of strain gauges gives better results than using a single strain gauge for determining critical stress intensity factor by the method of measuring strains in the vicinity of the crack tip. The work performed in this chapter paved ways to conduct dynamic experiments in the DCB specimen.

TABLE I Experimentally observed peak strain and associated  $K_{IC}$  for single and double strain gauge combinations and its comparison with  $K_{IC}$  obtained through closed form and numerical solutions

Expt No (i)	No of strain gauges (ii)	crack length mm (iii)	peak strain $\mu\epsilon$ (iv)	peak load N (v)	$K_{IC}$ exp Mpa $\sqrt{m}$ (vi)	$K_{IC}$ Analy. Mpa $\sqrt{m}$ (vii)	$K_{IC}$ Num Mpa $\sqrt{m}$ (viii)	% Diff vii-vi vi (ix)
LRG1	one	36.5	210	150	5.09	6.02	4.94	2.94
LRG2	one	36.5	123	160	2.98	6.42	5.24	75
LRG3	two	36.5	95	60	2.30	2.4	1.97	14.3
LRG4	two	36.5	168	100	4.07	4.01	3.29	19.2
LRG5	two	36.5	260	155	6.3	6.2	5.09	19.5

TABLE II Variations in experimental and numerical values of  $K_{IC}$  using single and dual strain gauges by Potty and Lovi

Potty/Lovi P LRG	ONE strain Gauge % variation	TWO strain Gauge %variation
P1 P2 P3	-18 -55 -45	-- -- --
LRG1 LRG2 LRG3 LRG4 LRG5	+2.94 +75.0 -- -- --	-- -- +14.3 +19.2 +19.5

## CHAPTER 2

DYNAMIC INTERLAMINAR STRESS INTENSITY FACTOR

---

## 2.1 INTRODUCTION

## 2.1.1 PRELUDE

One of the main mechanisms of failure in composite materials is delamination. As mentioned already in chapter 1 delamination is splitting of laminae into individual laminae under loading. Under impact loading, the problem is acute and it has been experimentally determined that a crack can propagate with a velocity as high as 300 m/s. The high speed crack propagation leads to the question - Whether dynamic interlaminar fracture toughness quite different from that of static.

The stress distribution at the tip of a crack propagating at high speed is different from the static crack due to introduction of time dependent terms. The equilibrium equations used as the basis for the computation of the static stress field are replaced by the equations of motion. The effect of high speed on stress distribution is more pronounced for crack velocity close to the Rayleigh wave. A Rayleigh wave is a surface wave and whose velocity is about 90 percent of the shear wave velocity.

## 2.1.2 LITERATURE SURVEY

Efforts have been put in to experimental evaluation of the dynamic fracture toughness of materials specially on isotropic metals. Several different kinds of dynamic loading techniques and recording equipment have been developed.

Kalthoff et. al [16-17] used a sharp edge load input into a precracked 3-point bend specimen. The falling knife-edge gave dynamic load input to the specimen. A series of shadow optical photographs were taken by the Cranz-Schardin 24 spark high speed camera. The load developed between the specimen and sharp edge determined by the post impact displacement showed an oscillating behavior with an overall increasing tendency. This was caused by eigenvibrations of the specimen that were excited by the impact process. It was seen that the stress intensity factors decrease for an advancing crack.

Rosakis et al [19] performed experiments on dynamic crack propagation using a wedge loaded DCB specimen of an austenitized, quenched and tempered 4340 steel. The dynamic stress intensity factor measurements were done by means of the optical method of caustics. The shadow spot patterns were photographed with a Cranz-Schardin high speed camera and the study was based on elastodynamic analysis. The dynamic stress intensity factor  $K_I^d$  was obtained as a function of crack tip velocity considering interaction of reflected shear and Rayleigh waves. The DCB specimen was made from a large plate and the

results are not of much relevance to the results of this work which employs slender cantilevers. The results show that the dynamic stress intensity factor is monotonically increasing function of crack velocity. At low speeds the dependence is small, but at high speeds it becomes quite pronounced.

Ravichandran and Clifton [20] developed a plate impact experiment for studying dynamic fracture process occurring under sub-microsecond loading. A disc containing a mid-plane, pre-fatigued, edge crack which had propagated half way across the diameter was impacted by a thin flyer plate of the same material. A compressive pulse propagated through the specimen and reflected from the rear surface as a step tensile pulse with a duration of 1 microsecond. This plane wave loaded the crack and caused initiation and propagation of the crack. The motion of the rear surface was monitored by the laser interferometer system. The location of the crack front was mapped before and after the experiment using a focused ultrasonic transducer.

Similar kind of work was carried out by Kalthoff et al.[18] who extended a preexisting crack in a DCB specimen by a wedge loading system. A series of six real shadow optical patterns were photographed by a Cranz-Schardin high speed camera. It was seen that the stress intensity factors decrease for an advancing crack.

Prasad [6] developed an experimental set-up to measure dynamic critical energy release rate in mode I. A DCB specimen of reinforced glass fabric was used with an artificial



precrack and was loaded dynamically in mode I. In this technique the upper cantilever was attached to a very rigid support and to the end of the lower cantilever, a long elastic round bar of 16 mm diameter was hanged. A drop weight around this bar (drop weight worked as a bead) impacted a stopper at the end to generate a tensile pulse, travelling all along the bar to the cantilever end, loads the specimen dynamically. The stress profiles of the loading pulse was measured through strain gauges bonded to the hanging bar and the crack velocities were determined by foil gauges bonded in front of the crack tip. The crack velocities were in the range of 20 to 100 m/s. At these crack velocities value of  $G_{IC}$  was found to be very small and specimen required large amount of work input to reach high run away crack velocities. Thus energy balance could not be achieved by him properly.

Babu [ 7 ] developed a technique to determine interlaminar critical energy release rate in mode II under impact loading conditions. A precracked ENF (end notched flexural) specimen was loaded in 3-point bending by a bar striker accelerated by a 19 mm bore air gun. The incident and the reflected pulse were recorded. These gave the load and the deflection of the specimen. Thin copper wires bonded in front of the crack tip were used to measure crack velocity. The limitation of the study was that the crack velocities were not measured accurately.

## 2.1.3 OUTLINE OF THE PRESENT WORK

In the present work, a new technique has been developed to experimentally evaluate the value of dynamic interlaminar stress intensity factors

High velocity crack propagation in a DCB specimen is imparted first by storing energy in both the cantilevers. The energy in the cantilevers is stored by bolting the two cantilevers together with a prenotched bolt just prior to the crack tip and pulling the cantilevers apart on a tensile machine. To release energy towards the crack tip the bolt is suddenly broken by a suitable mechanism. Dynamic stress intensity factor is determined by recording strain profiles on a side face of the specimen at two predetermined locations through strain gauges.

## 2.2 EXPERIMENTAL TECHNIQUES

### 2.2.1 INTRODUCTION

In this section details of the new technique of imparting high velocity to the interlaminar crack is discussed in detail. The preparation of the specimen, the system of releasing energy by a quick release mechanism, bonding of strain gauges and the strain measurements are described in this section.

### 2.2.2 SPECIMEN PREPARATION

The preparation of DCB specimen is similar to procedure discussed in chapter 1. It was modified by drilling a through hole of 4.5 mm ( $3/16$  " ) diameter and at a distance of 30 mm from the load application line (FIG. 2.1). As the cantilevers of the specimen were very hard (of the order of 33 on C-scale), the hole was drilled by a carbide tip drill.

The faces of the cantilevers to be bonded were prepared by rubbing them on a fine grit (220) emery paper for five minutes under light hand pressure. For bonding, epoxy LY 556 and hardener HY 951 was used in the ratio of 100:10 by weight. The sides of the cantilevers were covered with a layer of wax to prevent epoxy coating and the faces to be bonded were

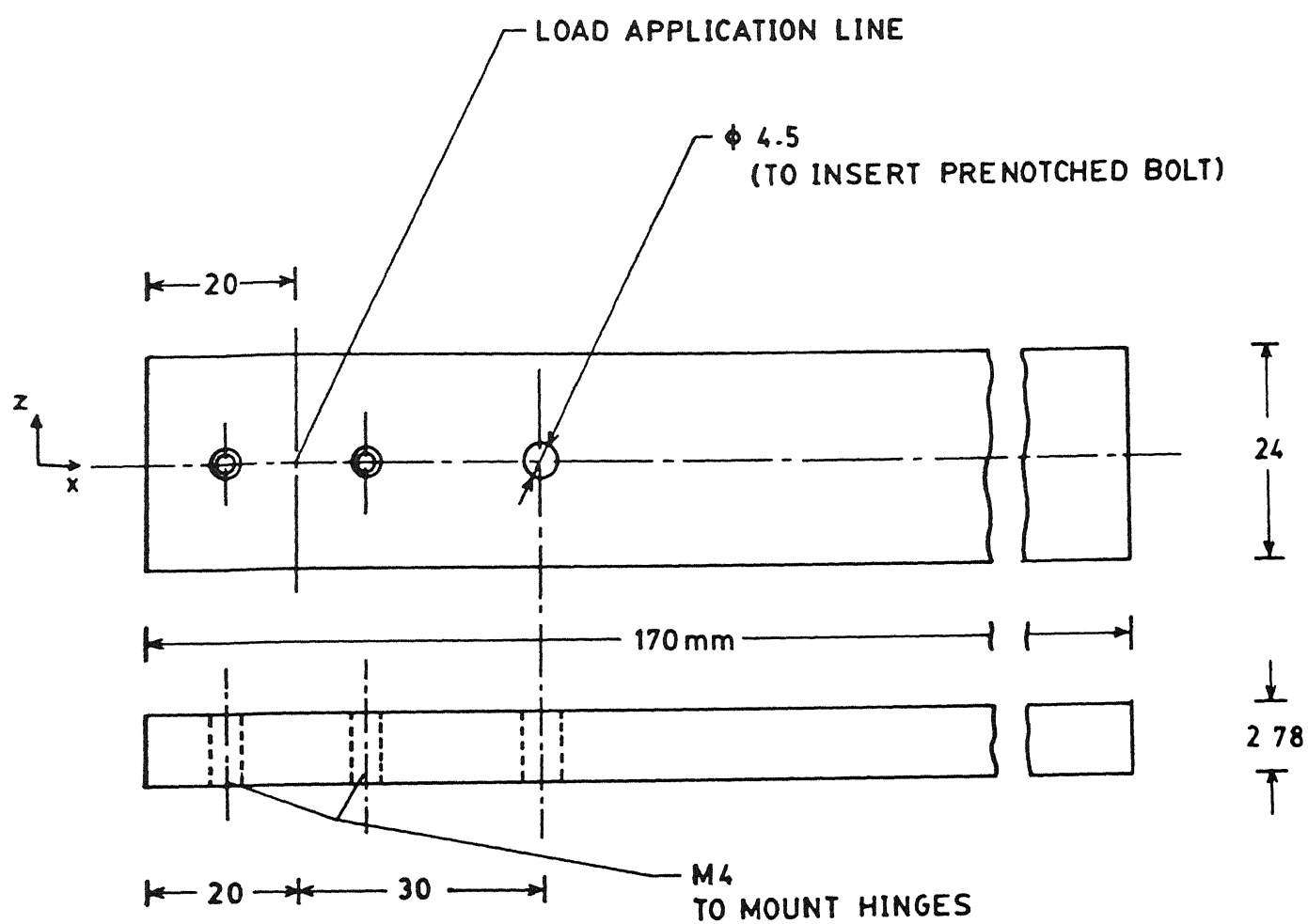


FIG. 2.1 A cantilever of DCB specimen.

cleaned with acetone of AR grade. The mixture of epoxy and hardener was applied thoroughly to the cleaned faces. The two strips were then put together and pressed in the bonding fixture. The bonding fixture discussed in chapter 1 was modified by drilling a hole of 45 mm in the bottom face and inserting a pin (FIG 22). This pin acts as a locating pin and also restricts the mixture of epoxy and hardener to gush into the holes drilled into the cantilevers. Between the strips and the flats of the fixture, a sheet of BOPP film was placed on each side. This film works as a release film.

The fixture along with the specimen was placed between two platens of a hydraulic press. The platens were heated through in built heaters and the temperature of the specimen was monitored by using a copper-constantan thermocouple. The temperature of the specimen was maintained at  $60^{\circ}\text{C}$  under 1 Mpa pressure for six hours. It was then allowed to cool down to the room temperature.

### 2.23 PREPARATION AND USAGE OF THE SYSTEM WHICH IMPARTS HIGH VELOCITY TO THE INTERLAMINAR CRACK

A system was designed and fabricated to instantaneously release the energy stored in the slender cantilevers of the DCB specimen. This is done by clamping two cantilevers together with a bolt and pulling the ends of the cantilevers on a tensile loading machine. This section explains the prenotched bolt, the arch, the arch aligning fixture and the

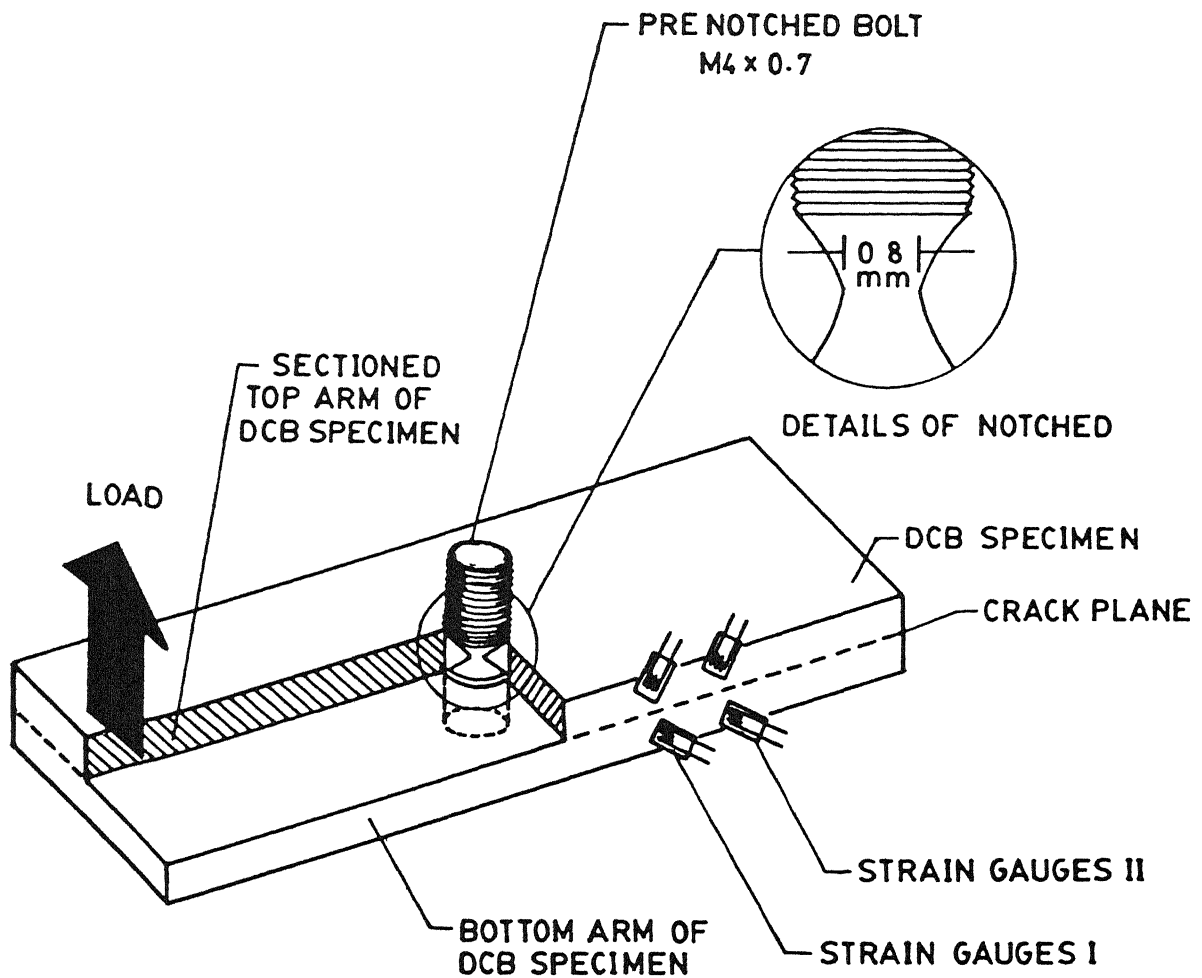


FIG. 2.2 Schematic sketch to represent position of notched bolt and Strain Gauges in a DCB specimen.

procedure in detail

#### PRENOTCHED BOLT

The allen head bolt of standard size M4\*07 (UNBRAKO) was used in the present work. This bolt was mounted on the lathe and a notch was cut into it. The dimensions of this notch were determined by a shadow graph with a magnification of 20. The bolt was then inserted through the hole (45 mm  $\phi$ ) in the cantilevers of the DCB specimen (FIG 22)

#### ARCH

Two arches (one each to be used on either side of the specimen) of mild steel were fabricated. The arch was used for resting of the nut and to distribute centre point load to sides as shown in fig 23a. Its details are shown in figure 23. The arch was designed so that,

- it absorbs a small inertia,
- it has a small bearing area at ends,

It had a central hole to pass the bolt through it. Special care was taken to make sure that the centre portion of the arch does not bow under load so much that it touches the specimen.

#### ARCH ALIGNING FIXTURE

The alignment of the arches on each side of the DCB specimen should be perfect because if they are not aligned, then the load on prenotched bolt will change from linear to a combination of both linear and flexural. Considering this

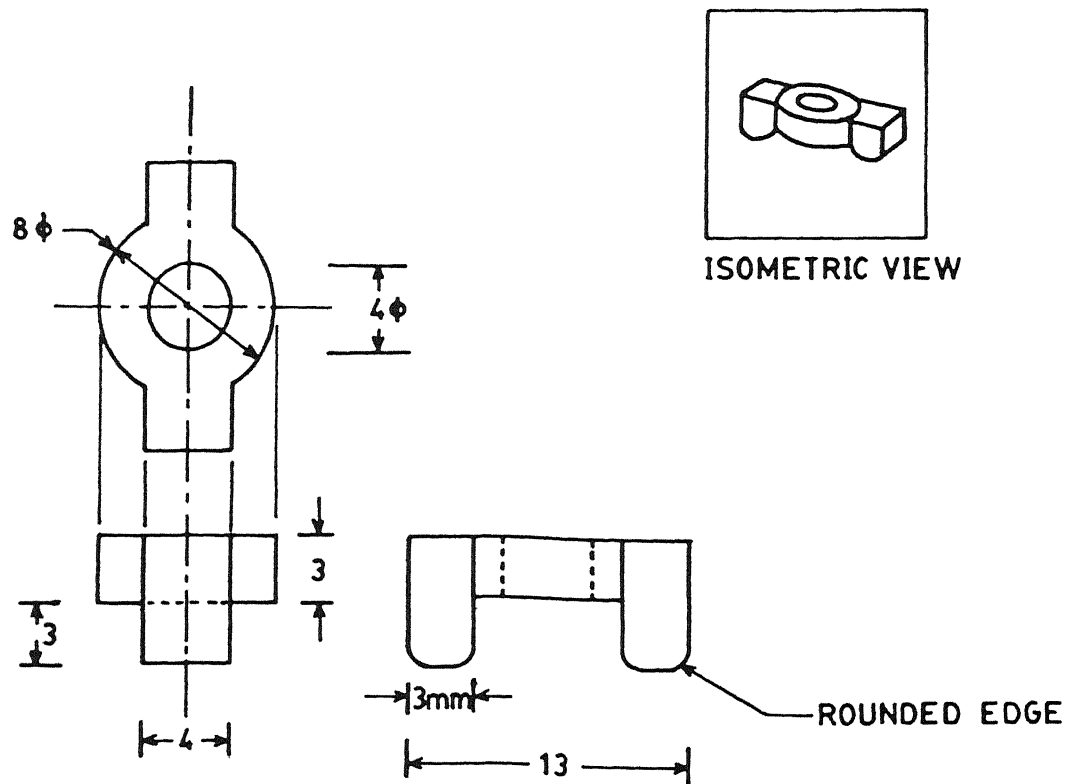


FIG. 2.3 ARCH



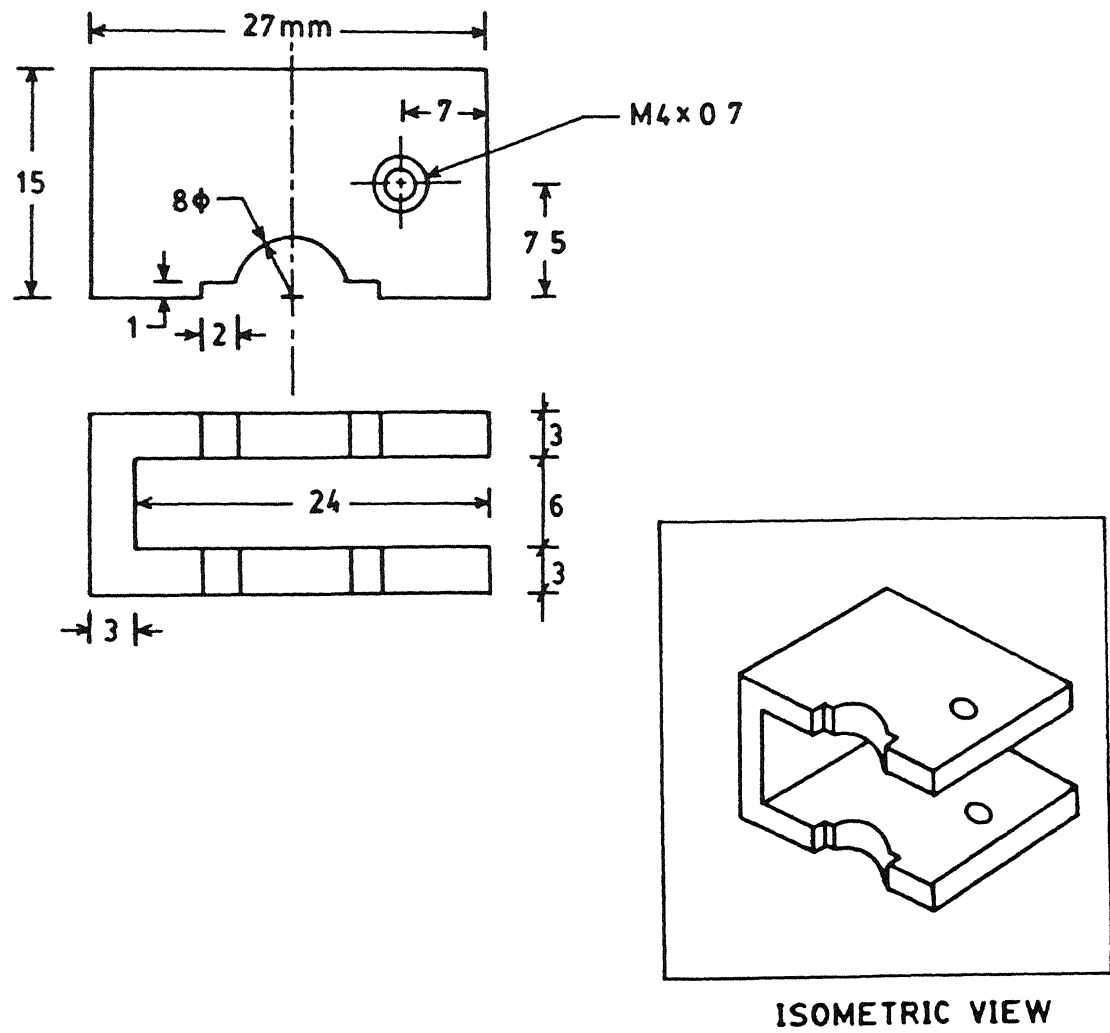


FIG. 2.4 Arch aligning fixture.

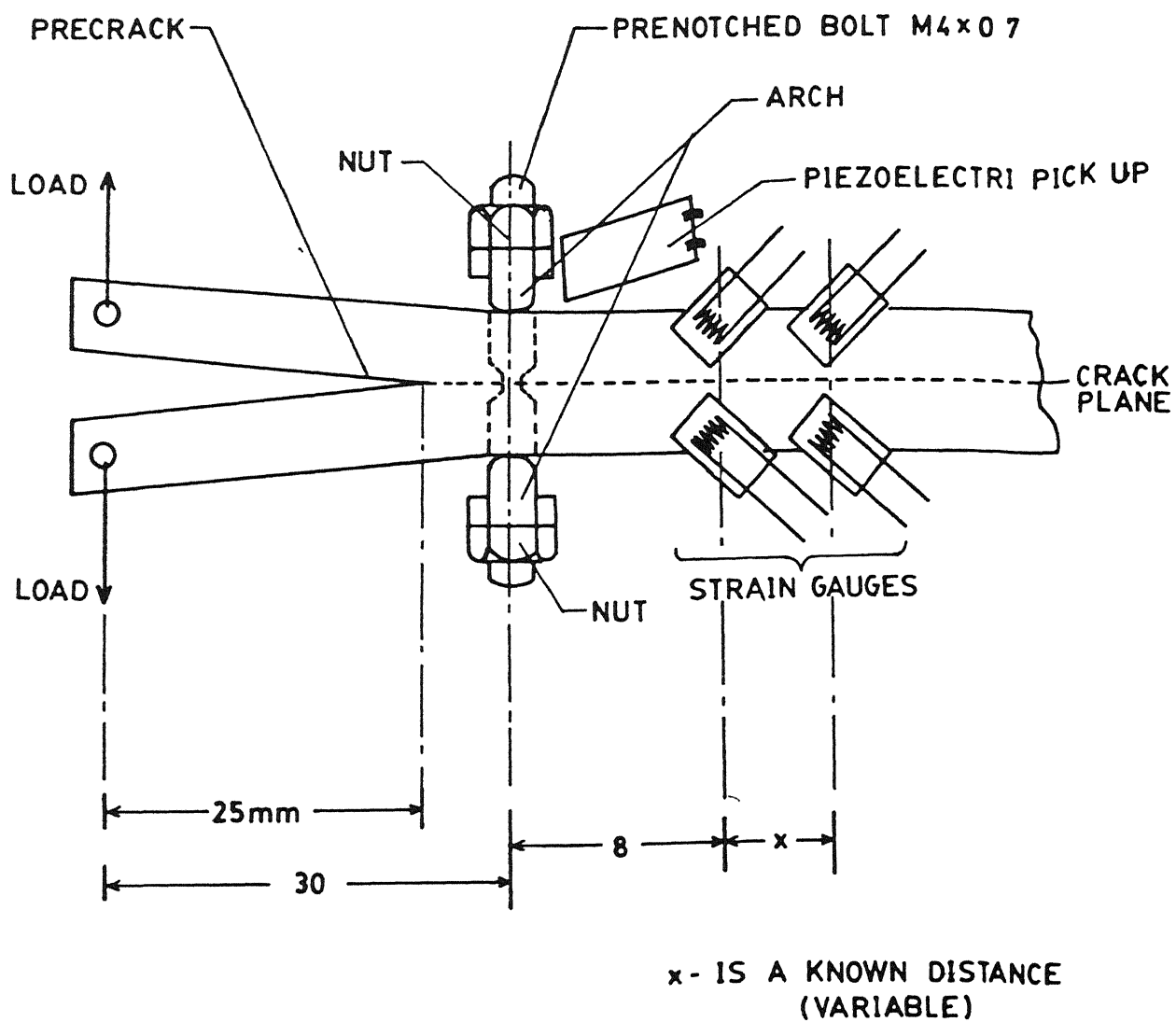


FIG. 2.5 Details of assembly.

factor, a fixture (FIG 24) was designed to align the bridges on both sides of the DCB specimen. This fixture enables perfect alignment of bridges while tightening of the nut on the prenotched bolt.

#### ASSEMBLY

The assembly was done as shown in figure 25. The nut was tightened enough on both sides so as to remove high spots between legs of bridges and surface of the DCB specimen.

#### PROCEDURE

The assembly was done as shown in figure 25 and the arms of the DCB specimen were loaded on an INSTRON machine. As the load reached the required value (300 N), the nut on the lower half was tightened by the spanner manually. This introduced a twisting torque in the prenotched bolt due to which it broke suddenly. This quickly released the energy stored in the cantilevers of the DCB specimen thus imparting high velocity to the interlaminar crack.

### 2.2.4 BONDING OF STRAIN GAUGES

The strain gauges similar to one used in chapter 1 are used for this study. The strain gauges have a gauge length of 0.2 mm and a gauge width of 15 mm. Details of the strain gauges are given in figure 14.

As the area on to which strain gauges are to be bonded is very small, extreme care is undertaken while bonding.

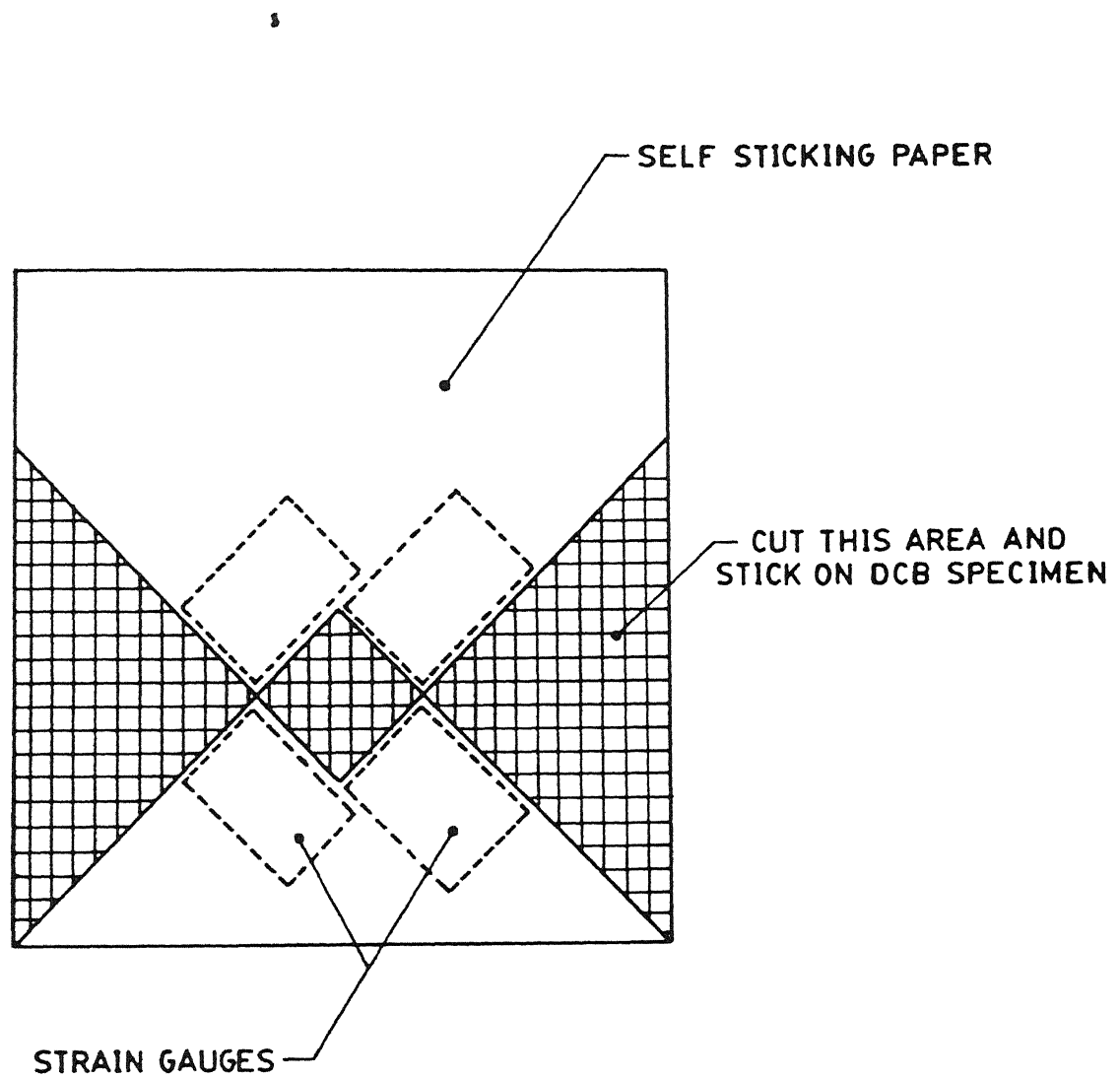


FIG 2.6 Strain Gauge mounting fixture.

them. Positioning of all the four strain gauges is done with the help of a fixture. This fixture is made by cutting the hatched area of a self sticking paper as shown in figure 2.6. The central square and the coexisting triangles provide a housing for all the four strain gauges. The section is stuck to the side face of the DCB specimen. The area lying under the fixture is thoroughly cleaned with acetone to degrease and remove dust particles. Epoxy LY 556 and the hardener HY 951 are used in the ratio 10:1 by weight. The mixture of epoxy and hardener is applied evenly to the strain gauge housing area. The ambient temperature is kept around 55 to 60<sup>0</sup> C for about 12 hours to help curing with the help of an infra red lamp. Localized pressure is also applied while curing takes place.

After the curing is over, to check the location and orientation, the bonded strain gauges are then placed under travelling microscope. Readings of microscope are taken and X,Y coordinates of the strain gauge base are recorded. This plot ensures the accuracy of the location and orientation of the strain gauges. It is seen that the center of gauges are within 0.05 mm from the prescribed location and the orientation is within a range of  $\pm 2^0$ .

## 2.2.5 MEASUREMENT OF STRAIN

The strain output is measured through an oscilloscope ( PHILIPS PM 3350 ). The oscilloscope is a dual channel hence it is capable of recording two signals at a time.

Triggering of the oscilloscope is done externally with the help of a piezoelectric pickup. In this work, a stereo needle is used as a triggering device ( FIG 25). This is placed just after the arch assembly so that when the prenotched bolt breaks, it triggers the oscilloscope. Two strain pulses are recorded on the oscilloscope screen. Both of these show a spike. The spike gives the peak strain encountered by the respective set of the gauges as the crack scoots under the set. Whereas the time lag between the spikes enables evaluation of crack velocity by knowing distance between two sets of gauges.

## 2.3 RESULTS AND DISCUSSIONS

### 2.3.1 INTRODUCTION

A DCB specimen with slender cantilevers (each made of hardened alloy steel and of thickness 2.78mm) was used in the present study. The cantilevers bonded by epoxy and with a precrack of 25mm from the load application point were held together with a prenotched bolt, 5mm away from the tip of the precrack. When the load was applied, crack front was extended to the prenotched bolt creating a sharp crack front. Two dual mirror image combinations of strain gauges were bonded to the sides of the specimen. The first combination (A) was placed 8mm from the center line of the prenotched bolt and the second combination (B) was placed 13mm from the prenotched bolt.

The load was then applied to the ends of the cantilevers and the energy was stored in them. This stored energy was suddenly released by breaking the prenotched bolt so as to have dynamic crack propagation.

### 2.3.2 EXPERIMENTAL RESULTS

A total of four experiments were conducted in this study. For each experiment, strain v/s time was recorded by a Philips storage oscilloscope. Details of each experiment are presented below.

(i) Experiment No LD1 This was the exploratory experiment done with a single combination of the strain gauges at location A. The cantilevers were pulled by a load of 162 N before the prenotched bolt was broken manually. The wave form obtained is shown in Fig 27. Being the first experiment the sensitivity of the vertical scale of the oscilloscope was kept low and therefore the strain was measured only on three levels with the peak strain of  $190 \mu\epsilon$ .

(ii) Experiment No LD2. This was done with two combinations of strain gauges with load on cantilever equal to 300 N. The recorded wave forms are shown in Fig 28. The strain pulse of A combination shows a peak strain of  $133 \mu\epsilon$  but B does not show a prominent peak. However, some disturbance of low magnitude, almost of the order of noise, was observed. It is believed that the crack tip did not reach up to B combination during the time window set on the oscilloscope. The recorded disturbances are believed to be caused by the breaking of the prenotched bolt.

(iii) Experiment No LD3. The cantilevers were loaded in this experiment to a load of 300 N. Similar behavior was shown by the strain wave form with a peak of  $135 \mu\epsilon$  by A combination of strain gauges whereas here also B did not show any clear signal.

(iv) Experiment No LD4 : The cantilevers were loaded to 300 N in this experiment before manually breaking the prenotched bolt. This was done with one strain gauge in A location and two in B location. Similar kind of peak was observed in the strain pulse



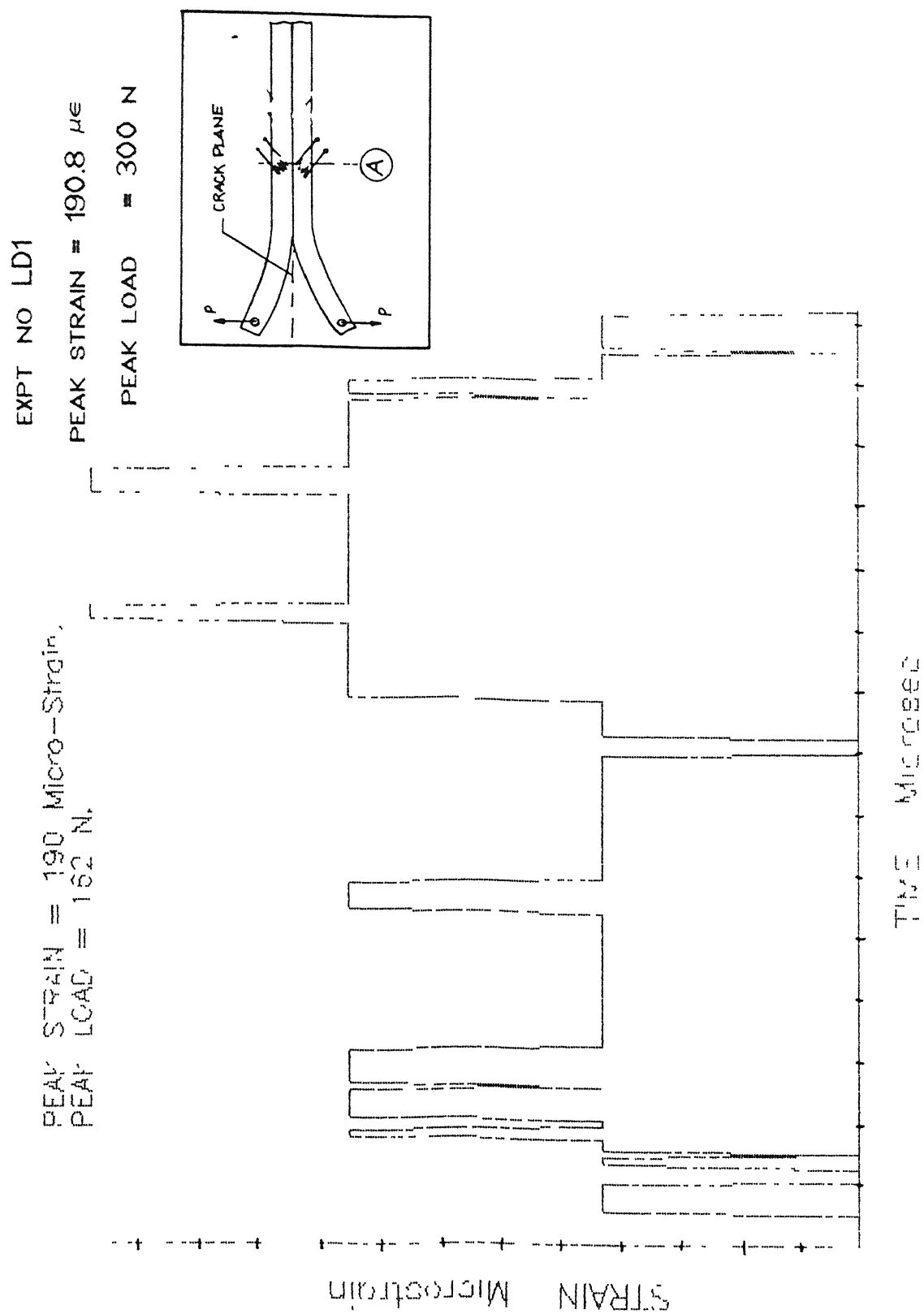


Fig. 2.7 Experimentally recorded Strain v/s Time for LD1

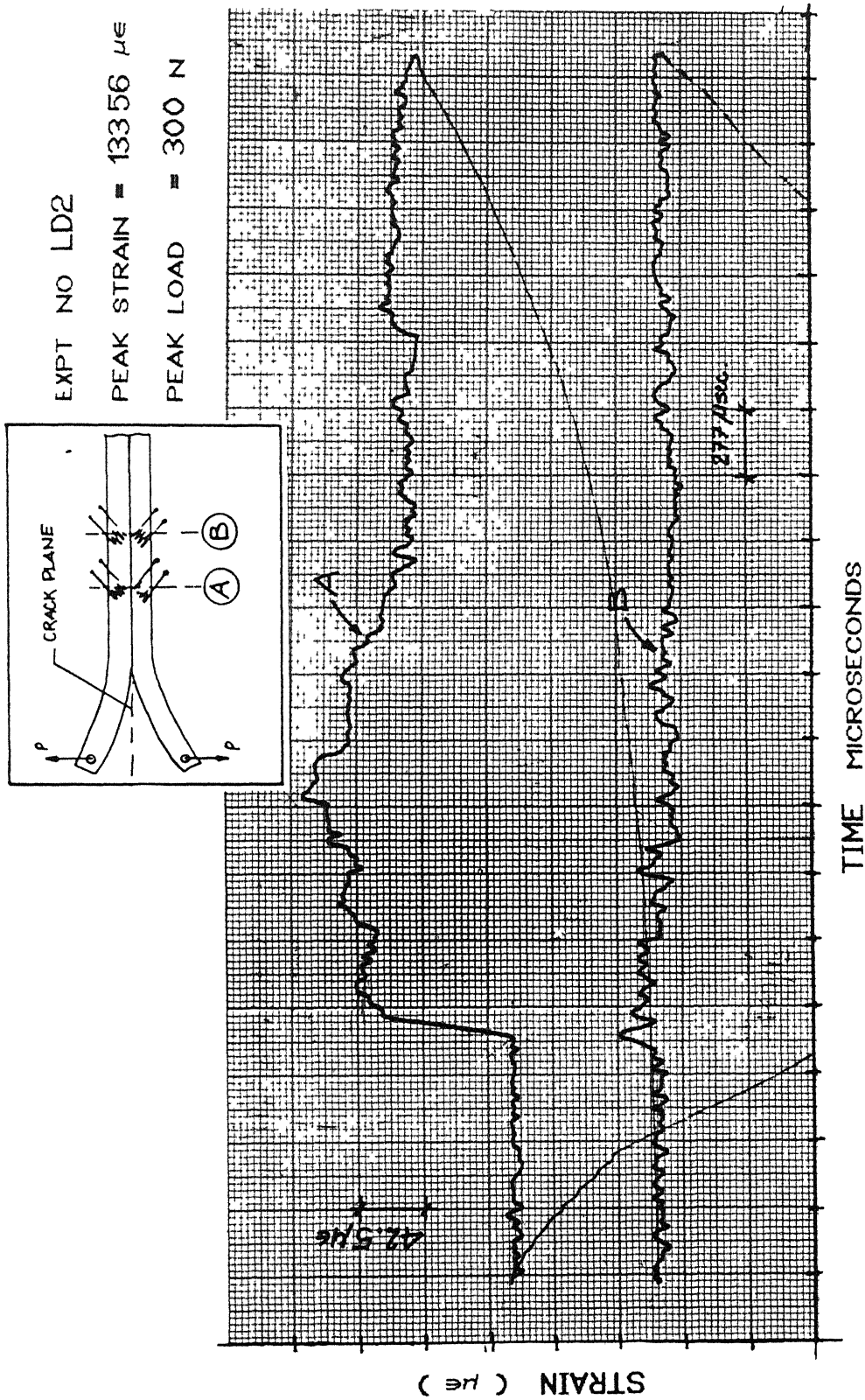


Fig. 2.8 Experimentally recorded Strain v/s Time for LD2

EXPT NO LD3

PEAK STRAIN = 13556  $\mu\epsilon$

PEAK LOAD = 300 N

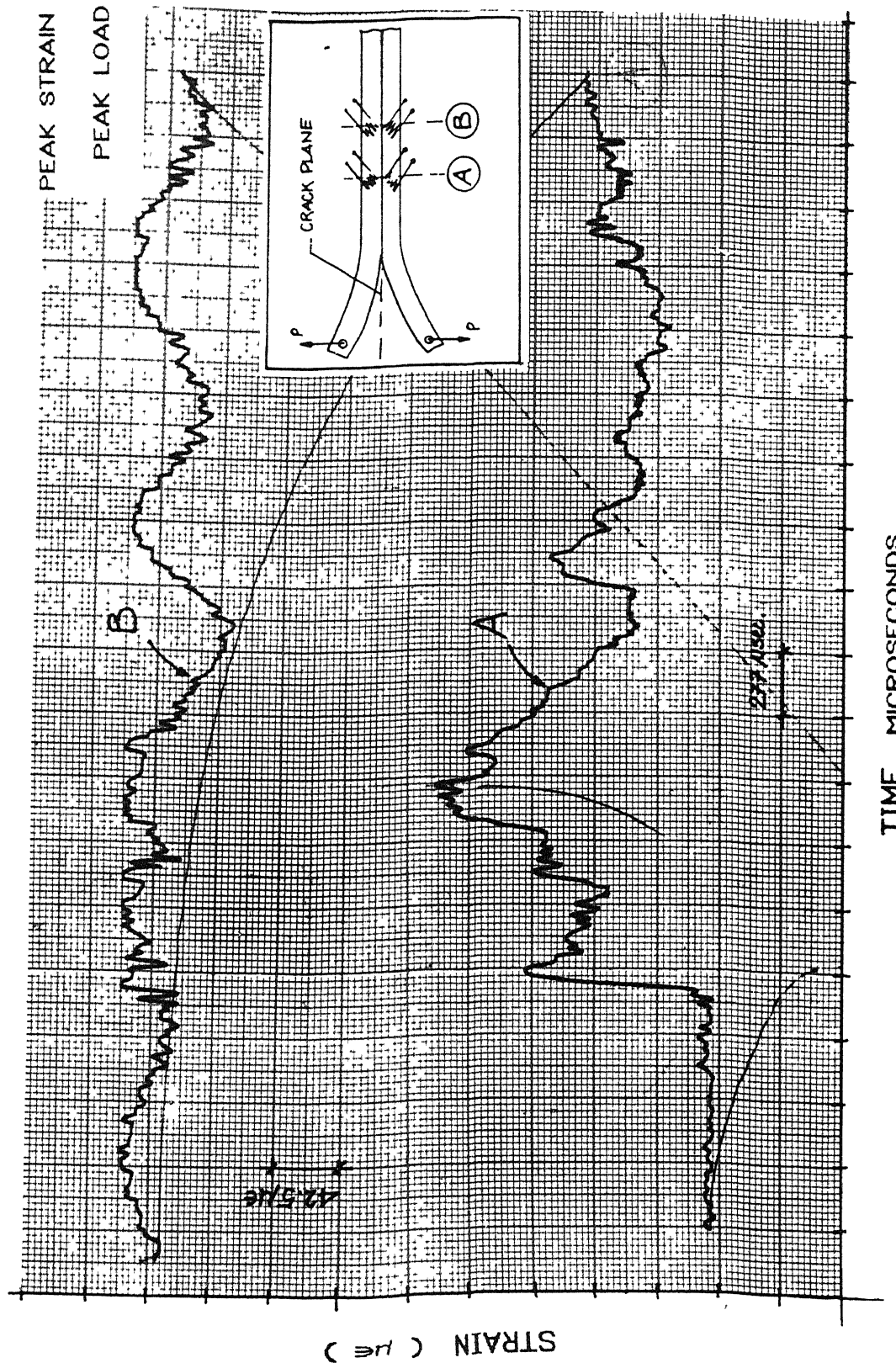


Fig. 2.9 Experimentally recorded Strain v/s Time for LD3

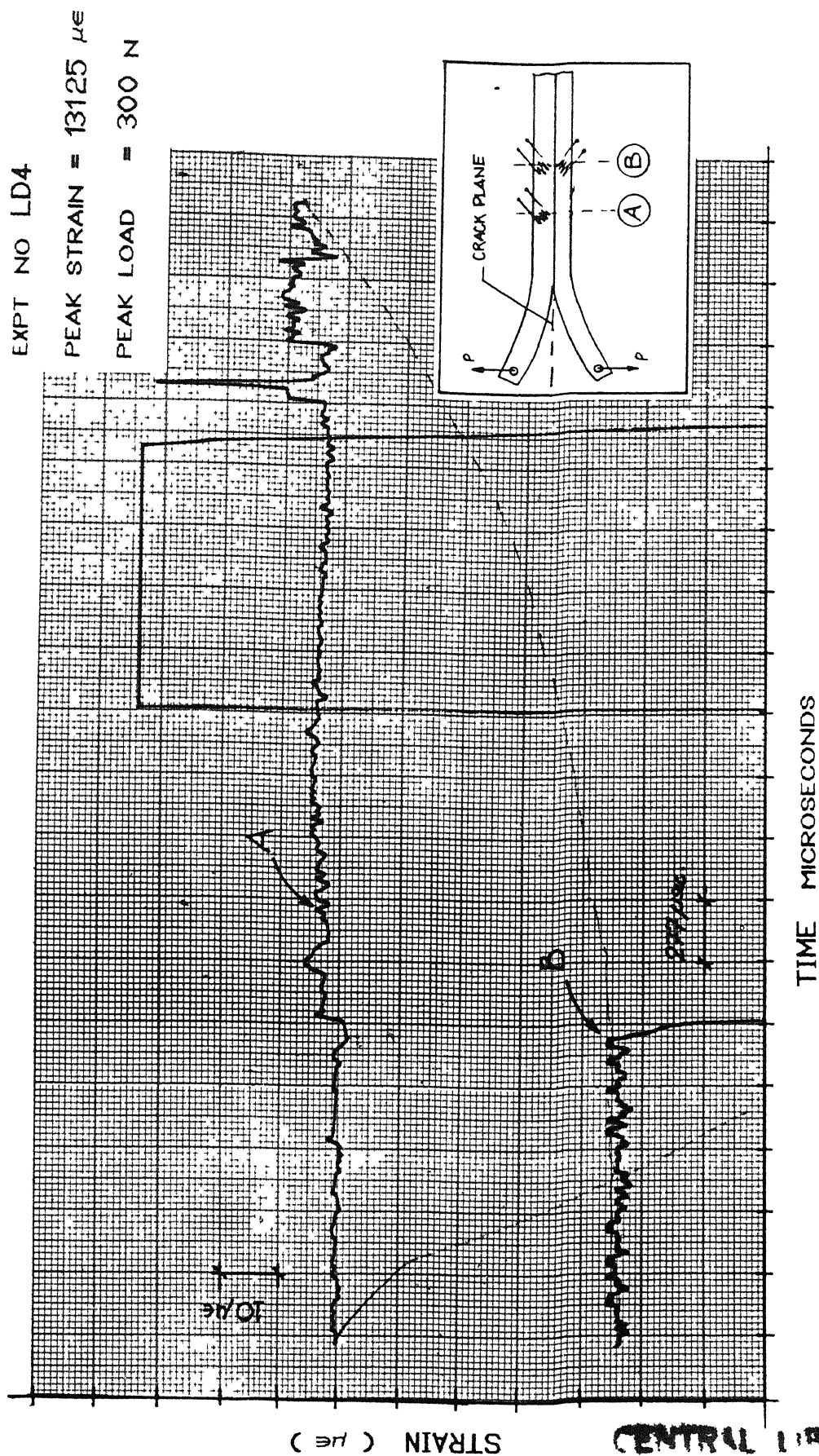


Fig. 2.10 Experimentally recorded Strain v/s Time for LD4

CENTRAL LIBRARY

114865

by the strain gauge at location A. Since only one strain gauge in spite of two recorded the pulse, the strain was half

As the B or rear combination of strain gauges did not record the pulse, the crack velocities were not measured. However, knowing the time window, it was supposed that the crack velocity was less than 14 m/s

The strain field does not change much if the crack velocity is less than 10 % of the shear wave velocity ( 2800 m/s in steel) [8]. Since the crack velocities in the study are much lower, the results of numerical technique [13] can be used to evaluate the critical dynamic intensity factor  $K_I^D$ . The dynamic stress intensity factors were evaluated by strain pulses recorded at A and is tabulated in Table III

### 2.3.3 COMPARISON WITH QUASI-STATIC CRACK PROPAGATION

In the quasi-static crack propagation the experimental stress intensity factors obtained using two strain gauges were 2.3, 4.07, 6.3 (MPa $\sqrt{m}$ ) with an average of 4.22 MPa $\sqrt{m}$ . The dynamic crack propagation studies led to the dynamic stress intensity factors of 4.62, 3.24, 3.28, 3.18 (MPa $\sqrt{m}$ ) with an average of 3.58 MPa $\sqrt{m}$ .

### 2.3.4 ANALYSIS OF SLOW CRACK GROWTH

The critical energy release rate, based on quasi-static work [14], is of the order of 10 J/m<sup>2</sup> which is quite small. But, one should also know how much energy is stored in

the cantilever arms used in this study before it is released for crack growth. Under the load,  $P$ , on the cantilever ends the deflection,  $\delta$ , is well known as

$$\delta = \frac{4Pl^3}{Eb^3h} \quad (21)$$

Where  $l$  is the length of cantilever (crack length in this case),  $E$  is Young's Modulus,  $h$  is the thickness of cantilever and  $b$  is the width. The strain energy stored in both the cantilevers is given by

$$U = P\delta = \frac{4P^2l^3}{Eb^3h} \quad (22)$$

For a typical value of  $P = 300$  N,  $U$  is 0.09 J. Based on the quasi-static  $G$ , the crack needs 0.002 J which is much smaller than the stored energy. However, because of other unaccounted parameters such as cantilevers acquiring kinetic energy, the full amount of released energy is not likely to be available for crack growth. Furthermore, 0.09 J energy is quite small. Therefore, it is understandable that crack moves with a very low velocity.

It may be worthwhile to explore how to impart more energy for crack growth. Also, it is worth noting that loads on the cantilever ends cannot be increased much because the bending moment on the cantilever will be large enough to cause yielding. Therefore load  $P$  in equation 22 would be expressed in terms of stress of the outermost plane of the cantilevers. As we know

from eq 22 that the energy stored in both the cantilevers is given by

$$U = \frac{4}{Fb} \left(\frac{l}{h}\right)^3 P^2$$

also using,

$$\sigma = My/I = \frac{bh}{6l} \sigma \quad (23)$$

substituting this in energy equation we get

$$U = \frac{bhl}{9E} \sigma^2 \quad (24)$$

Equation 24 clearly indicates that the energy stored per unit width of the cantilever is directly proportional to crack length (l) and the cantilever width (h). Thus having more crack length and more thickness of specimen, more energy can be stored imparting much more crack velocity.

TABLE III Experimentally observed Peak Strain and associated Dynamic stress intensity factor  $K_I^D$  for 365mm crack length

Expt No (i)	No of Strain gauges used (ii)	PEAK STRAIN $\mu\epsilon$ (iii)	$K_I^D$ MPa $\sqrt{m}$ (iv)	Average MPa $\sqrt{m}$ (v)
LD1	Two	190 8	4 62	3 58
LD2	Four	133 56	3 24	
LD3	Four	135 68	3 28	
LD4	Three	131 25	3 18	



#### 2.4 CONCLUSIONS AND SUGGESTIONS FOR FUTURE WORK

The work has been carried out to experimentally determine dynamic stress intensity factor by measuring strain near the crack tip through a combination of strain gauges in a DCB specimen with slender cantilevers. The specimen was loaded in mode I on an INSTRON machine under displacement controlled conditions. As the load was applied the energy gets stored in the arms of the DCB specimen. After loading it to a known load the prenotched bolt acting as an energy barrier was broken. This sudden release in energy resulted in dynamic crack propagation and as the crack moved under the strain gauges a pulse was sensed by the combination of the gauges. The strain pulse was recorded at location A only because the crack was moving at a very slow speed ( at  $> 14$  m/s ) and by the time the crack has moved to location B the time window of oscilloscope might have ended. Thus the dynamic stress intensity factor was calculated by the peak strain of A location.

Further work can be carried out using a larger crack length and thick cantilevers of the DCB specimen. As explained in section 2.3.4 this will result in more energy storage imparting higher velocity to the crack front.

The limitation of the technique mentioned in the present study is that, high crack velocities may not be possible unless one choose very thick cantilevers. But then the study

does not correspond to DCB specimen with slender cantilevers and the mechanism of delamination is not simulated by using thick cantilevers

For further study one might go for loading the DCB specimen by impact. This can be performed easily by using bullets from an air gun or by dropping weight method. These can be done in more controlled environment as well as this may impart very high velocities to the crack tip.

2

3

## REFERENCES

- 1 NTakeda, R.L.Sierakowski, C A Ross & L E Malvern,  
 -Delamination crack propagation in ballistically impacted glass/epoxy composite laminates,  
 -Experimental Mechanics, 22, (1982) pp 20-5.
- 2 Prashant Kumar, D K.Sarkar, S.C Gupta,  
 -Rolling resistance of elastic wheels on flat surface,  
 -Wear, 126, (1988), pp 117-129
- 3 Wilkins D J, J R.Eisenmann, R A Camin, W.S Margolis & Benson,  
 -Characterising delamination growth in graphite epoxy,  
 -Damage in composite materials, ASTM STP, 775, (1982), pp 168
- 4 Han K S & J.Koutsky,  
 -The interlaminar fracture energy of glass fibre reinforced polyester composite,  
 -J.Comp.Materials, 15, (1981), pp 371-388
- 5.Devil D F, R A.Schapery & W.L Bradley,  
 -A method for determining the mode I delamination fracture toughness of elastic and viscoelastic composite materials,  
 -J Comp Materials, 14, (1980), pp 270-285.
- 6 Prasad J S R K T,  
 -Experimental evaluation of dynamic interlaminar  $G_{IC}$  of glass fabric reinforced epoxy laminates,  
 -MTech Thesis, (1990), IIT, Kanpur
- 7 Babu Suresh K,  
 -Experimental studies on dynamic  $G_{IIc}$  of interlaminar crack propagation in CFRP,  
 -MTech Thesis, (1991), IIT, Kanpur
- 8 David Broek,  
 -Elementary Engineering Fracture Mechanics,  
 -Martinus Nijhoff Publishers.

9 Williams ML.,

- The stress around a fault or crack in a dissimilar media,
- Bull of Seismo Soc of America, 49, 2, (1959), pp 199

10 Sun CT & Jih C.J.,

- On strain energy release rates for interfacial cracks in bi-material media,
- Engg Fract Mech, 28, No. 1, (1987), pp 13-20.

11. Shukla A, Agrawal BD & Bharat Bhushan,

- Determination of stress intensity factor in orthotropic composite materials using strain gauges,
- Engg Fract Mech, 32, No 3, (1989), pp 469-477.

12 Nadarjah N, Shukla A & Letcher S,

- Application of fiber optic sensors to fracture mechanics problems,
- Engg Fract. Mech, EFM-MS 688, (1991)

13 Verma S.K., Prashant Kumar, Kishore NN,

- A finite element software for finding strain field around the crack tip for computing stress intensity factors,
- Manuscript under preperation

14. Potty Keshvan P.K.,

- Experimental and FEM investigation of SIF in DCB specimen,
- MTech Thesis, (1992), IIT, Kanpur

15 Freund LB,

- Crack propagation in an elastic solid subjected to general loading constant rate of extension,
- J Mech Phys Solids, 20, (1972), pp 129-140.

16. Kalthoff J.F, S Winkler & Beinert J.,

- The influence of dynamic effects in impact testing,
- Int J Fract, 13, (1977), pp 528-531.

17. Kalthoff J.F, W.Bhome, Winkler S & Klemm W.,

- Measurements of dynamic SIF in impacted bend specimen,
- CSNI specialists meeting on power research Institute, Palo Alto, Calif., Dec 1-3, (1980), pp 1-17

18 Kalthoff J.F, Winkler S & J Beniart,

- Dynamic SIF for arresting cracks in DCB specimen,  
-Int J Fract , 12, (1976), pp 317-319
- 19. Rosakis A J, Duffy J & Freund L B.,  
-The determination of dynamic fracture toughness of AISI 4340  
Steel by shadow spot method,  
-J Mech Phys. Solids, 32, No 4, (1984), pp 443-460
- 20. Ravichandran G., Clifton R J,  
-Dynamic fracture under plane wave loading,  
-Int J Fract , 40, (1989), pp 157-201

\*\*\*\*\*

ME-188.3-M GUN-EX